



Allometric growth and intraspecific variation of the craniomandibular bones of *Tarbosaurus bataar* (Theropoda, Tyrannosauridae): a geometric morphometric approach

CHAN-GYU YUN, RAFAEL DELCOURT AND PHILIP JOHN CURRIE

LETHAIA



Since it was first described in 1955, many fossils of the tyrannosaurid theropod *Tarbosaurus bataar* have been recovered from the Upper Cretaceous Nemegt Formation of Mongolia and its contemporaneous units in east Asia. Among these, there were individuals of different sizes and stages of maturity, but not much research has been done on the changes that occurred during the growth of this dinosaur. In this work, growth trajectories in the shape of various, individual craniomandibular bones of *Tarbosaurus bataar* are examined through geometric morphometrics. Several major changes in craniofacial anatomy are observed through the growth series, including increases of the relative heights of the dentary, jugal, maxilla, and nasal; the transition of the lacrimal from a T-shape to a 7-shape; negative allometric growth in the anteroposterior length of the orbit; increased sizes of the cornual processes of the postorbital and the ventral flange of the jugal; broadening of the frontal accompanied by an enlargement of the dorsotemporal fossa; and widening and thickening of the nuchal crest so that the mid-length of the parietal appears relatively narrower. Such results indicate the main allometric shape change patterns in craniomandibular anatomy of *Tarbosaurus bataar* were broadly congruent with those of other tyrannosaurids, particularly with *Tyrannosaurus rex*. It is assumed that many of these changes were related to disproportionate increase of the bite forces and strengthening the skull structure during growth. Additionally, a significant amount of variation appears to be uncorrelated with size, suggesting that *Tarbosaurus bataar*, like other theropod dinosaurs, had significant intraspecific variation in craniomandibular anatomy. □ *Dinosauria*, *Evolution*, *Ontogeny*, *Development*, *Skull*, *Tyrannosaurus rex*, *Tarbosaurus bataar*.

Chan-gyu Yun ✉ [changyu1015@naver.com], Independent Researcher, Incheon 21974, Republic of Korea; Rafael Delcourt [rafael.delcourt@gmail.com] Department of Biology, Universidade de São Paulo, Ribeirão Preto, Brazil; Philip John Currie [philip.currie@ualberta.ca], Department of Biological Sciences, University of Alberta, Edmonton, Alberta, T6G 2E9, Canada; manuscript received on 09/10/2024; manuscript accepted on 10/07/2025; manuscript published on 03/10/2025 in Lethaia 58(4).

Tarbosaurus bataar is a large tyrannosaurid theropod found in the upper Cretaceous (?Maastrichtian) Nemegt Formation of Mongolia, and the Subashi Formation of China. Fragmentary large tyrannosaurid remains from other upper Cretaceous units of eastern Asia may be referable to this taxon (Currie 2003a, b; Holtz 2004). Some specimens of this taxon were initially referred to as a species of the genus *Tyrannosaurus* (Maleev 1955a). *Tyrannosaurus bataar* was based on a large skull (PIN 551-1) from the Nemegt Formation. In a nearly simultaneous publication, Maleev (1955b) described *Gorgosaurus lancinator*, *Gorgosaurus novojilovi* and *Tarbosaurus efremovi* based on three specimens (PIN 553-1, 552-2, and 551-2 respectively) from the same area, as he considered that differences in overall sizes, dimensions of the skulls, shapes of the orbits, and proportions of the postcranial skeletons were sufficient to distinguish

them from *Tyrannosaurus bataar* and from each other. However, Rozhdestvensky (1965) recognized these taxa represent an ontogenetic series of a single taxon (in which *Tyrannosaurus bataar* has priority). Furthermore, he introduced the new combination *Tarbosaurus bataar* for this Mongolian tyrannosaurid as he considered it to be different enough to be classified as a distinct genus from the North American *Tyrannosaurus*.

The work of Rozhdestvensky (1965) was among the first to describe the dramatic ontogenetic changes in cranial and postcranial anatomy of tyrannosaurids, from juveniles with slender bauplans, gracile skulls with labiolingually narrow teeth to adults with robust bauplans, deep skulls and robust teeth. Since then, growth changes in cranial and skeletal anatomy of tyrannosaurids have been thoroughly described, particularly focusing on North American

taxa (Russell 1970; Carr 1999, 2020; Currie 2003a, b; Carr & Williamson 2004; Voris *et al.* 2019, 2022; Funston *et al.* 2021; Yun 2023). After the description and naming of this taxon, many additional specimens of *Tarbosaurus bataar* have been recovered, and pertain to different stages of growth (Hurum & Sabath 2003; Brusatte *et al.* 2010, 2012a; Tsuihiji *et al.* 2011; Currie 2016; Jerzykiewicz *et al.* 2021; Yun *et al.* 2022; Lee *et al.* 2023).

Despite this wealth of specimens, however, little has been described about the morphological changes that occurred in the growth of *Tarbosaurus bataar* since Rozhdestvensky (1965), who briefly described the changes in skeletal proportions and increases in ‘robusticity’ of several bones. This is partly due to the fact that although large numbers of *Tarbosaurus bataar* have been discovered, very few have been described (Hurum & Sabath 2003; Brusatte *et al.* 2010; Currie 2016; Jerzykiewicz *et al.* 2021; Lee *et al.* 2023). Although specimens that pertain to early stages of ontogeny (two-to-three-year-olds) of this taxon have been described (Currie & Dong 2001; Tsuihiji *et al.* 2011), individuals that represent ‘intermediate’ growth stages between small juveniles and large adults have not been described since the mid-20th century (Maleev 1955a, b, 1974). As such, Tsuihiji *et al.* (2011) suggested that the ontogenetic trajectory of *Tarbosaurus bataar* was very similar to that of any North American tyrannosaurid. This is based on the fact that two-to-three-year-old individuals of *Tarbosaurus bataar* (e.g. MPC-D 107/7) show many similarities to immature individuals of North American taxa. However, these specimens do not provide quantitative evidence as it is difficult to compare individuals corresponding to the ontogenetic stages between very young offspring and adults. Currie (2003a) and Delcourt (2016) used different-sized *Tarbosaurus bataar* individuals for their bivariate and morphometric analyses respectively, but their studies mainly focused on interspecific patterns. Yun *et al.* (2022) described ontogenetic allometry of the frontal bone of *Tarbosaurus bataar*, but this study involved only a single cranial element. Furthermore, recent studies have demonstrated that there is a considerable amount of intraspecific variation that is unrelated to growth that is prevalent among non-avian dinosaurs, which may significantly affect our knowledge about their palaeobiology (Carpenter 2010; Scannella & Horner 2011; Smyth *et al.* 2020). Individual variations in skeletal morphologies of North American tyrannosaurids have been thoroughly described (Carpenter 1990; Currie 2003b; Carr 2020; Paulina-Carabajal *et al.* 2021; Warshaw & Fowler 2022), but again, little has been investigated about Mongolian *Tarbosaurus*

bataar in this respect. The lack of descriptions regarding allometric, ontogenetic or intraspecific variation of *Tarbosaurus bataar* has even led some scholars to consider several individuals (e.g. PIN 552-2) as distinct taxa (Carpenter 1992; Olshevsky & Ford 1995), in spite of the work of Rozhdestvensky (1965). However, most workers on Tyrannosauridae still consider these specimens to represent *Tarbosaurus bataar* (Carr 1999; Currie 2003a, b; Holtz 2004).

Geometric morphometric analysis, a method that quantifies and visualizes shape variation through homologous landmarks (and the semi-landmarks between them) keeps the morphological information in the form of Cartesian coordinates (Bookstein 1991; O’Higgins & Johnson 1988; Polly 2018). This has proven to be particularly useful in evaluating allometric and ontogenetic changes in living and past organisms, including non-avian dinosaurs (Campione & Evans 2011; Maiorino *et al.* 2013; Ratsimbaholison *et al.* 2016; Knapp *et al.* 2021; Hedrick 2023). Indeed, this approach is considered superior to the traditional morphometric method based on multivariate analysis of several measurements. First, it can capture the geometric information that is involved in the shape variation of biological individuals, which is often ignored in traditional morphometrics. Thereby, it is able to sieve subtle variations in morphology that are not easily summarized by simple measurements (Rohlf & Marcus 1993; Brusatte *et al.* 2012b; Cooke & Terhune 2015; Wang & Fang 2023), although this potentially makes it more susceptible to taphonomic deformation (Kammerer *et al.* 2020). Furthermore, geometric morphometrics itself is designed to complement traditional morphometrics (Adam *et al.* 2013; Cooke & Terhune 2015; Wang & Fang 2023), in that it allows a comprehensive assessment of shape, and produces easy visualization of major shape changes (Hedrick 2023). Based on these advantages, the geometric morphometric approach is increasingly being applied to studies of macroevolution, ontogeny, sexual dimorphism, and systematics of various organisms (Bhullar *et al.* 2012; Adams *et al.* 2013; Cooke & Terhune 2015; Foth *et al.* 2016; Hedrick 2023; Wang & Fang 2023).

So far, only a few geometric morphometric studies include information about ontogenetic variation of tyrannosaurids, including *Tarbosaurus bataar*. And even in these cases, the main focuses are about the macroevolution of Archosauria or Saurischia on broad scales (Bhullar *et al.* 2012; Foth *et al.* 2016; Plateau & Foth 2020; Lautenschlager 2022), or compare ecomorphologies of pairs of different theropod clades (i.e., Ceratosauria and Tyrannosauoidea; Delcourt 2016). Furthermore, only the overall shapes

of the entire skulls were used in these studies, and as such the detailed changes in each bone that compose the skulls were not revealed.

In this work, allometric shape changes in *Tarbosaurus bataar* are described using the geometric morphometric approach, using individual craniomandibular bones from different sized individuals. Additionally, this provides an opportunity to demonstrate, and describe the variations within them that are not related to differences in the sizes of the animals.

Material and methods

The morphological variations in 11 craniomandibular bones of *Tarbosaurus bataar* are analysed through two-dimensional geometric morphometrics by plotting 2D landmarks and semi-landmarks on published photographs, rigorous reconstructions, and unpublished images of some specimens using the programs tpsDIG and tpsUtil (Rohlf 2015, 2017a, b). Scale bars were used to scale each digitized specimen. The semi-landmarks were plotted following the protocol of Ma *et al.* (2020), which involves drawing the curves between the landmarks, resampling these curves through tpsDIG, and changing them to landmarks by tpsUtil. Landmarks are placed at the intersection endpoints of the sutural surfaces of different bones, or at the maxima or endpoints of the curvature (e.g. fenestra, fossa), while semi-landmarks are placed along edges or curves between adjacent landmarks, with equal distances along a dotted outline, following the procedures used in previous studies (e.g. Bookstein 1991; Cooke & Terhune 2015; Foth *et al.* 2016). Due to inaccessibility of many specimens within exhibit mounts, as well as postmortem damage, obscured sutural surfaces in articulated specimens, or the underdevelopment of key characteristics in immature

individuals (e.g. cranial ornamentations), some bones with complex structures, such as the nasal or surangular, had to be analysed only by their lateral contours. This suggests that potentially valuable three-dimensional information could be obscured. However, based on the criteria presented by multiple previous studies analyzing ontogenetic and allometric changes in craniomandibular anatomy of non-avian dinosaurs (Campione & Evans 2011; Maiorino *et al.* 2013, 2015; Foth *et al.* 2016; Ratsimbaholison *et al.* 2016), most key allometric growth changes can still be assessed with a simplified two-dimensional approach. Table 1 and Supplementary Online Material 1 provides a number of specimens that are used for analyses of each cranial bone, and sources of the images used in this study. Visualization and descriptions of the positions of each landmark and semilandmark are provided in Figure 1 and Supplementary Online Material 2.

The generated coordinates of landmarks and semi-landmarks are superimposed using the function ‘Procrustes fit’ through the program MorphoJ (Klingenberg 2011) to generate a covariance matrix. Superimposing landmark coordinates minimize variations that are caused by non-shape factors such as position or rotation (e.g. Brusatte *et al.* 2012b; Foth & Rauhut 2013). And then, the generated covariance matrices are subjected to Principal Component Analysis (PCA), also using MorphoJ (Klingenberg 2011). The data from all landmarks and semi-landmarks are summarized into a series of Principal Component (PC) scores that condense the shapes of each image, and describe major shape variations through morphospace.

Additionally, to assess overall allometric shape changes, regression analyses of Procrustes coordinates onto log centroid sizes (CS, a proxy for size in geometric morphometrics that is equal to the square root of the summed square distances between all landmarks

Table 1. List of craniomandibular elements, number of specimens, landmarks and semi-landmarks used in this study. See Supplementary Online Material 1 for more details.

Element	View	Number of specimens	Number of Landmarks	Number of semilandmarks
Premaxilla	Lateral	6	5	6
Maxilla	Lateral	13	8	36
Nasal	Lateral	7	4	12
Lacrimal	Lateral	9	5	17
Jugal	Lateral	8	10	11
Postorbital	Lateral	8	6	18
Quadratojugal	Lateral	8	4	8
Frontal	Dorsal	5	10	40
Parietal	Dorsal	4	6	38
Dentary	Lateral	7	4	23
Surangular	Lateral	5	7	33

and their centroid; Mitteroecker *et al.* 2013) are performed on each of the bones (permutation tests with 10,000 rounds). A growth pattern is considered allometric, or provisionally allometric, when the p-value of each analysis is significant ($p < 0.05$) or marginally significant ($0.05 \leq p < 0.1$). Furthermore, the first two PCs that summarize most of the shape variations are regressed onto log CS as well. This determines which shape variations are strongly associated with size, and if so, how much size changes account for that variation. When the p-value of each analysis is lower than 0.05 or above 0.05 but below 0.1, allometric growth is considered to have significantly, or marginally contributed to the variation respectively. The regression analyses were performed in MorphoJ (Klingenberg 2011). MorphoJ and tps files including all shapes and analyses, are provided as Supplementary Online Material 3. Figures are generated through MorphoJ (Klingenberg 2011) as well as Adobe Photoshop CS4 software.

The anatomical nomenclature used in this study follows Currie (2003b), Carr *et al.* (2005, 2017), Carr (2020), Voris *et al.* (2022), Yun *et al.* (2022) and Sharpe *et al.* (2025).

Institutional abbreviations

AMNH, American Museum of Natural History, New York, USA; BYU, Brigham Young University Museum of Paleontology, Utah, USA; LACM, Natural History Museum of Los Angeles County, Los Angeles, USA; LH, Long Hao Institute of Geology and Palaeontology, Inner Mongolia, China; MPC (=GIN, GI SPS), Institute of Paleontology, Mongolian Academy of Sciences, Ulaanbaatar, Mongolia; PIN, Palaeontological Institute of Russian Academy of Sciences, Moscow, Russia; TMP, Royal Tyrrell Museum of Palaeontology, Drumheller, Canada; UMNH, Natural History Museum of Utah, Salt Lake City, USA; ZPAL, Institute of Palaeobiology, Warszawa, Poland.

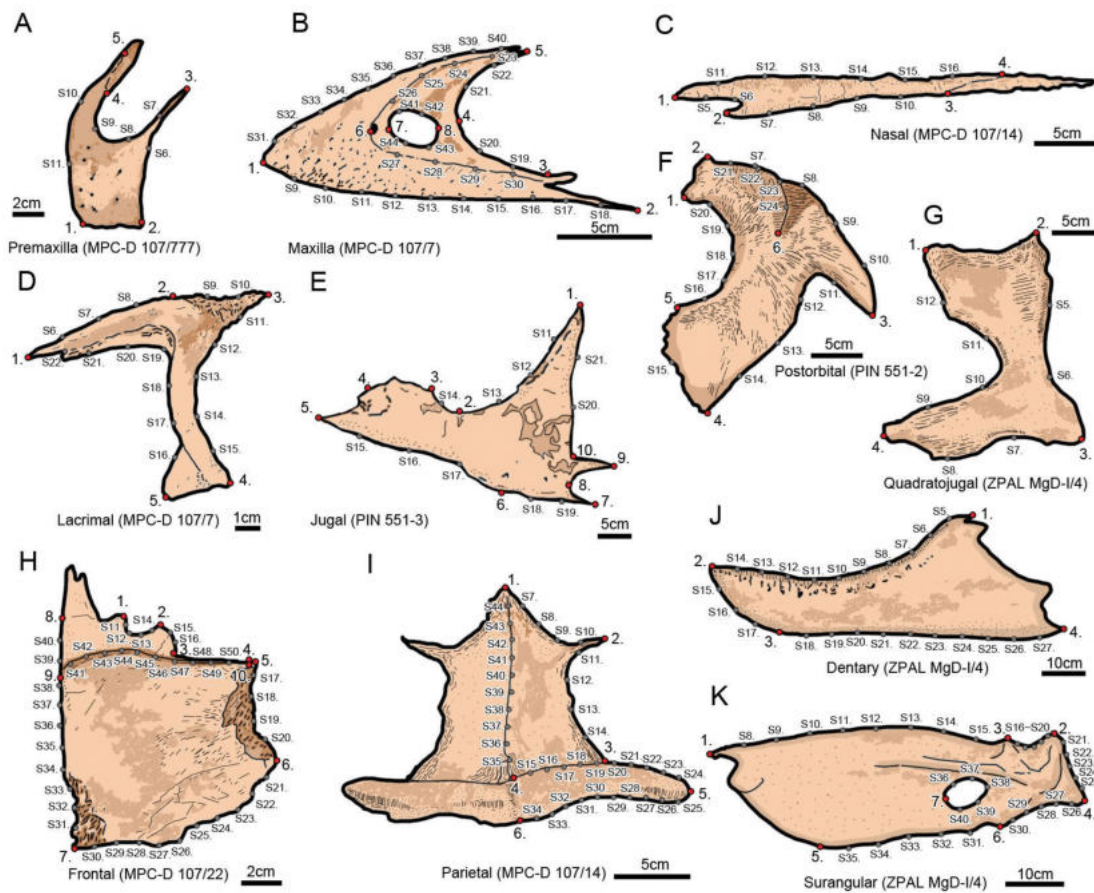


Fig. 1. Illustrations of the landmarks and semi-landmarks positions on the craniomandibular bones of *Tarbosaurus bataar*. Landmarks are shown as red dots, whereas semi-landmarks are marked with a 'S' and are shown as grey. See Table 1 and Supplementary Online Material 1, 2 for details.

Taxonomic referral

Because the Nemegt Formation (and potentially its contemporaneous strata) have multiple tyrannosaurid taxa other than *Tarbosaurus bataar* (*Alioramus remotus*, potentially *Bagaraatan ostromi* and *Raptorex kriegsteini*), referral of the specimens analysed in this work to *Tarbosaurus bataar* has to be justified. Known taxa of Alioramini, including *Alioramus remotus*, are characterized by numerous synapomorphies including an extremely elongated rostrum, increased tooth count, distinct knobs on the nasal, and a laterally projecting accessory hornlet on the jugal (Brusatte *et al.* 2012a; Foster *et al.* 2022). None of these features are present in specimens analysed in this work. *Raptorex kriegsteini* is a controversial tyrannosaurid taxon because of the immature status of the holotype, which lacks mature apomorphies (Fowler *et al.* 2011). However, it may be distinct from *Tarbosaurus bataar* as it possesses some unique characteristics, including

an extremely thin and straight ventral ramus of the lacrimal, a distinct, flange-like suborbital ligament scar of the lacrimal, and unusually tall anteroventral ala of the lacrimal (Carr 2022). Except in cases where the lacrimal is not preserved, this unique combination of features is not observed in any specimen analysed in this study. Lastly, *Bagaraatan ostromi* is another Nemegt taxon known from a very small juvenile and may differ from *Tarbosaurus bataar* in having two surangular foramina (Słowiak-Morkovina *et al.* 2024). Such a character is not seen in any of the specimens analysed in this work. Of note, many of the craniomandibular features that might be perceived as autapomorphic for *Raptorex kriegsteini* or *Bagaraatan ostromi* may not be sufficient to sustain the validity of these taxa, considering the substantial degree of ontogenetic and intraspecific variation in tyrannosaurids (see discussion; e.g. Fowler *et al.* 2011; Słowiak-Morkovina *et al.* 2024). Based on these reasons, we

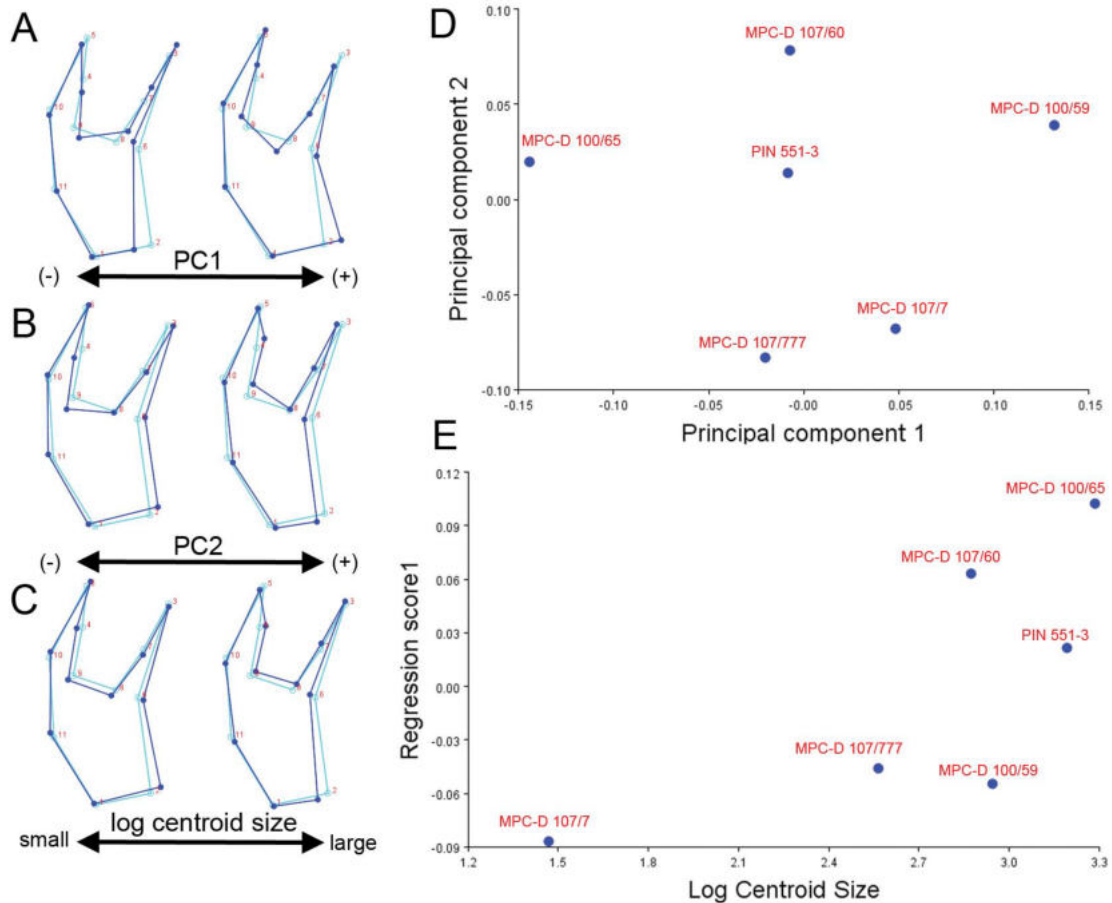


Fig. 2. *Tarbosaurus bataar* premaxilla shape analysed using geometric morphometrics. A, major changes in shape on PC1. B, major changes in shape on PC2. C, allometric analysis by multivariate regression of shape on log CS. D, two-dimensional morphospace defined by PC1 and PC2. E, scatter plot of regression scores against log CS. Red numbers indicate landmarks and semi-landmarks positions. Light blue wireframes represent the mean of variation, and dark blue wireframes represent major shape variation.

conservatively refer all the specimens analysed in this work to as a single taxon, *Tarbosaurus bataar*, following previous identifications (e.g. Currie & Dong 2001; Currie 2003a; Hurum & Sabath 2003; Carr 2005; Tsuihiji et al. 2011; Delcourt 2016; Yun et al. 2022). However, we acknowledge that the variation within the current hypodigm of *Tarbosaurus bataar* should be thoroughly examined in the near future, accompanied by extensive descriptions and assessments of the taxonomy of numerous undescribed specimens that are only provisionally referred to this taxon (see discussion; e.g. Hurum & Sabath 2003; Currie 2016; Jerzykiewicz et al. 2021; Lee et al. 2023).

Results

Premaxilla

The regression of Procrustes coordinates onto log centroid size (CS) for *Tarbosaurus bataar* premaxillae shows that 19.3% of the variance is predicted by size ($n = 6$), but this result is not statistically significant ($p = 0.4117$). A small premaxilla has an anteroposteriorly elongate body of the bone, an anteroventrally elongate external naris, an elongate, dorsoventrally shallow nasal process that is inclined backwards, and deep base of the maxillary process (Fig. 2). Large premaxillae have relatively short bodies, short external nares that have shifted posterodorsally, dorsoventrally deep, but short nasal processes, and dorsoventrally shallow maxillary processes (Fig. 2).

The PCA resulted in the first two PCs accounting for the 78.7% of the total variation (PC1 = 53.1%, PC2 = 25.6%). Negative values of PC1 are associated with the short premaxillary body, an external naris that is short and has shifted posterodorsally, a short but deep nasal process, and a shallow maxillary process. Positive values of PC1 describe the anteroposteriorly elongate body of the bone; anteroventrally elongate external naris; a shallow and anteroposteriorly elongate nasal process that is inclined posteriorly; and a broad maxillary process. PC1 mostly describes the variation in the relative length of the premaxilla as well as the length and the anteroposterior breadth of the maxillary process (Fig. 2). Variations described by negative and positive values of PC2 are broadly similar to those of positive and negative values of PC1. However, in positive values of PC2, the ventral part of external naris slopes posteroventrally, whereas negative values of PC2 are inclined horizontally. The largest proportion of variation explained by PC2 appears to be in the depth of the nasal process (Fig. 2).

The regression analysis of the PC1 score against log CS suggests 14.4% of PC1 can be explained by centroid size ($p = 0.4130$). The regression of PC2 onto log centroid size shows that 42.7% of this component is explained by the size of the bone, and it has slightly more statistical power compared to PC1 regression ($p = 0.1562$). Although neither result is statistically significant, it is provisionally assumed that the allometric variation is a subset of the much greater variations explained by PC1 and PC2. The wireframe graphs describing the shape differences between specimens with low and high log CS values are generally similar to the shape changes associated with low and high scores of these PCs. Indeed, there seems to a weak tendency that larger specimens plot in negative PC1, positive PC2 regions within the morphospace (Fig. 2).

Maxilla

Regression analysis of Procrustes coordinates onto log CS for *Tarbosaurus bataar* maxillae reveals that 29.0% of the variance is predicted by size ($n = 13$), and the permutation test indicates the presence of significant allometric growth ($p = 0.0013$). In each small maxilla, the anterior body and the jugal ramus of the bone are shallow, and the maxillary fenestra is well-separated from the anterior and ventral margins of antorbital fossa. Additionally, the alveolar and anterior margins of the bone are nearly straight, and the angle between them is relatively low (Fig. 3). In a large maxilla, both the anterior body and the jugal ramus are dorsoventrally deep, both the anterior and alveolar margins of the bone are convex, and together they meet at a higher angle, and the maxillary fenestra approaches the anteroventral corner of the antorbital fossa (Fig. 3).

The first two PCs explain over 67.8% of total shape variation (PC1 = 45.7%, PC2 = 22.1%). Negative values of PC1 describe a shallow anterior body and jugal ramus; nearly straight alveolar margin; gently inclined, relatively straight anterior margin that meets the alveolar margin at a shallow angle; and a maxillary fenestra that is well separated from the anterior and ventral margins of the antorbital fossa. Positive PC1 scores describe a dorsoventrally deep anterior body and jugal ramus; a convex anterior margin that is steeply inclined; a convex alveolar margin; and a maxillary fenestra that approaches the anterior and ventral margins of the antorbital fossa. Overall, PC1 is most closely related to the relative size of the antorbital fossa and the convexity of the alveolar margin (Fig. 3). Negative and positive values of PC2 describe the variations that are largely similar to those explained by corresponding values of PC1, except that the alveolar margin of the bone is relatively convex, and the dorsal

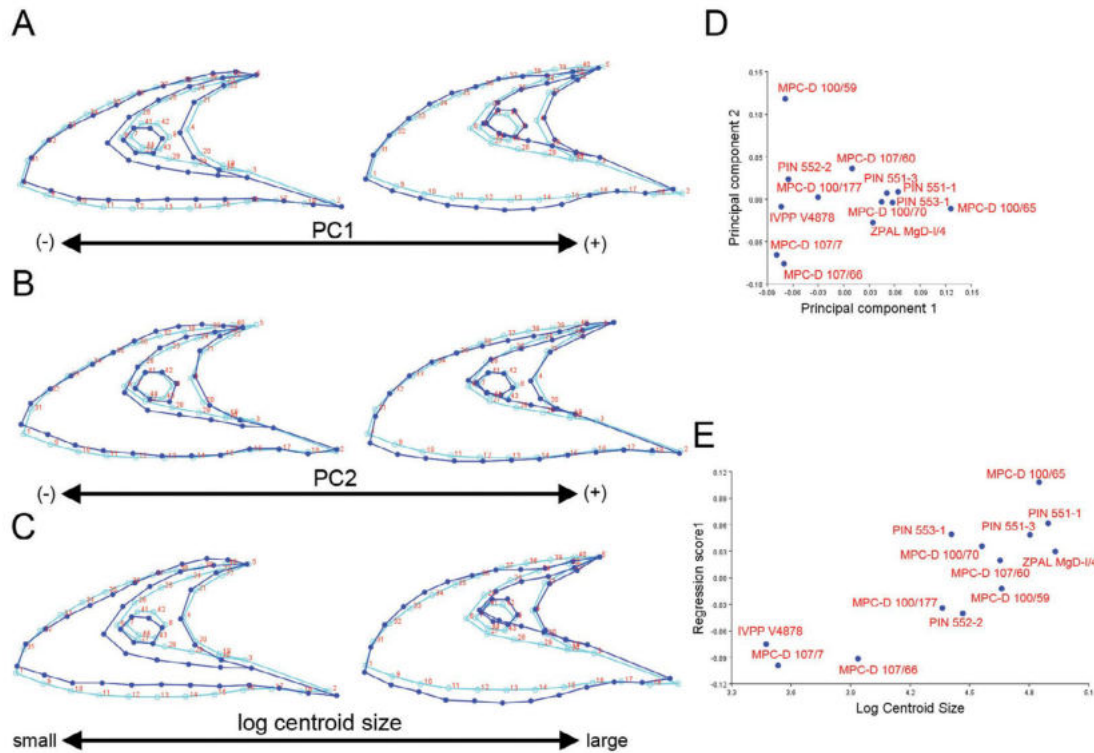


Fig. 3. *Tarbosaurus bataar* maxilla shape analysed using geometric morphometrics. A, major changes in shape on PC1. B, major changes in shape on PC2. C, allometric analysis by multivariate regression of shape on log CS. D, two-dimensional morphospace defined by PC1 and PC2. E, scatter plot of regression scores against log CS. Red numbers indicate landmarks and semi-landmarks positions. Light blue wireframes represent the mean of variation, and dark blue wireframes represent major shape variation.

margin of the ascending process is relatively convex in low PC2 scores; the convexity in the alveolar margin are most pronounced at anterior region in high PC2 scores; and the maxillary fenestra approaches the ventral margin of the antorbital fossa in high PC2 scores. Most of PC2 is related to whether the antorbital fossa is located relatively anteriorly or posteriorly (Fig. 3).

The regression analysis of the PC1 score against log CS reveals that size explains about 51.0% of PC1, and this correlation is significant ($p = 0.0050$). In contrast, it is revealed that only 21.4% of PC2 is explained by size, and their relationship is not statistically significant ($p = 0.1169$). Indeed, the majority of the large maxillae are clustered in the greater PC1 morphospace (Fig. 3).

Nasal

The regression of Procrustes coordinates onto log CS for *Tarbosaurus bataar* nasals reveals that 32.3% of the variation is explained by size ($n = 7$), and a correlation between shape and size is marginally significant ($p = 0.0537$). In each small nasal, the body of the bone

is dorsoventrally shallow, and its maxillary facet and dorsal margin are relatively straight. Additionally, both the premaxillary and subnasal processes are short, and the external naris is anteriorly positioned. Finally, the lacrimal facet (line between landmarks 3 and 4; Fig. 1, Supplementary Online Material 2) is elongate (Fig. 4). In a large nasal, the bone is deep, and its dorsal margin is convex. Both the premaxillary and subnasal processes are elongate, and in the case of the latter the process is shallow. The posterior end of the external naris has shifted backwards, and the maxillary facet is deeply concave. Finally, the lacrimal facet is short (Fig. 4).

In the PCA, the first two PCs represent approximately 79.5% of the total variation (PC1 = 41.1%, PC2 = 38.4%). Negative values of PC1 describe short premaxillary and subnasal processes; a shallow and anteriorly positioned external naris; a straight maxillary facet and dorsal margin of the bone; short lacrimal facet; and a shallow body of the bone. Positive values of PC1 describe a deep external naris in which its posterior end has shifted backwards; elongate premaxillary and subnasal processes; a convex dorsal

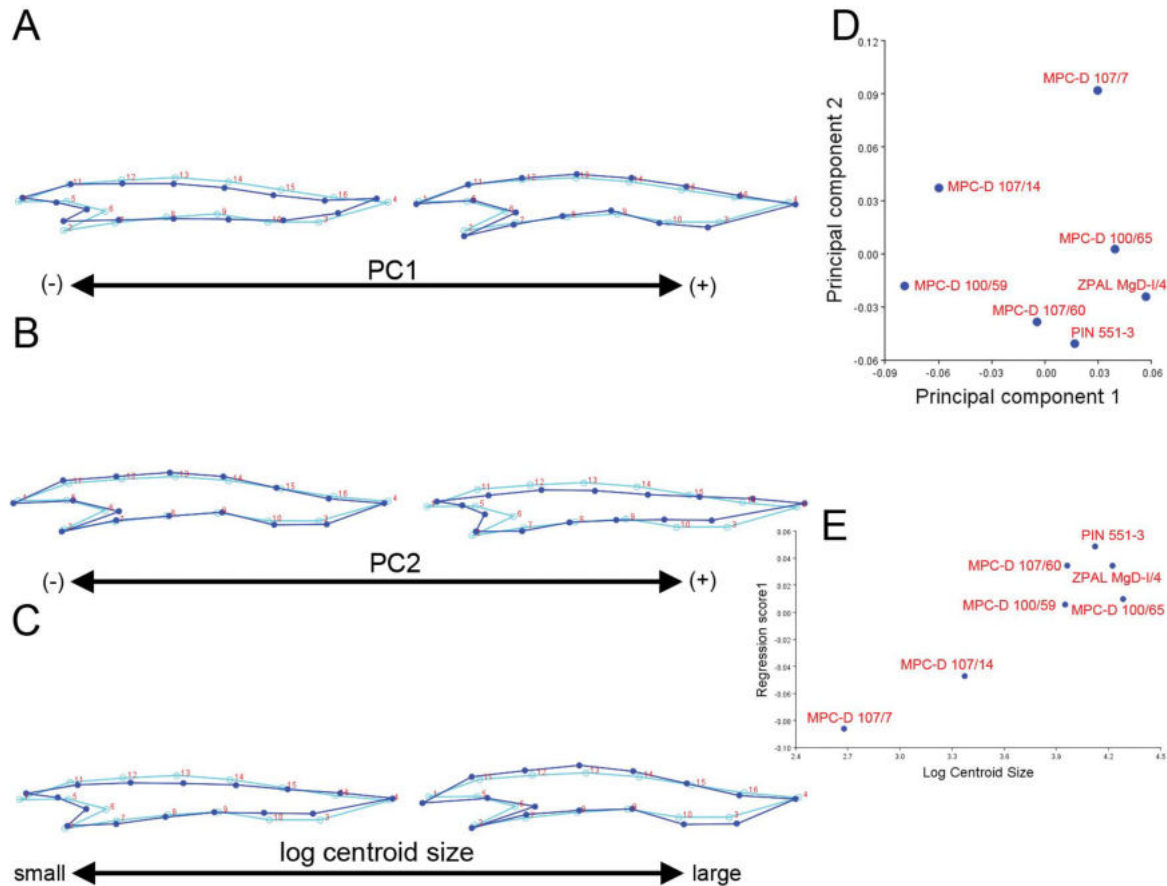


Fig. 4. *Tarbosaurus bataar* nasal shape analysed using geometric morphometrics. A, major changes in shape on PC1; B, major changes in shape on PC2; C, allometric analysis by multivariate regression of shape on log CS; D, Two-dimensional morphospace defined by PC1 and PC2; E, the scatter plot of regression scores against log CS. Red numbers indicate landmarks and semi-landmarks positions. Light blue wireframes represent the mean of variation, and dark blue wireframes represent major shape variation.

margin of the bone; a deeply concave maxillary facet; an elongate lacrimal facet; and a deep body. The largest variation explained in PC1 is in the position of the lacrimal facet (Fig. 4). In negative and positive values of PC2, the wireframe graphs are broadly similar to those of positive and negative values of PC1, except that the subnasial process is deeper; the premaxillary process is shallower; the lacrimal facet is elongate in positive values of PC2; and the subnasial process is shallower, and the lacrimal facet is shorter in negative values of PC2. Among the variations explained in PC2, the most significant is whether the most posterior part of the external naris is relatively more anterior or posterior (Fig. 4).

The regression analysis of the PC1 score against the log CS shows only 2.5% of PC1 is explained by the size, and its correlation is not significant ($p = 0.7690$). On the contrary, the regression of PC2 onto log CS suggests size explains more than 79.1% of PC2, and this is statistically significant ($p = 0.0169$). As expected, large

nasals are differentiated from small ones at negative PC2 values (Fig. 4).

Lacrimal

A regression analysis of Procrustes coordinates onto log CS for *Tarbosaurus bataar* lacrimals shows that 35.4% of the variation is explained by size ($n = 9$), and its statistically significant nature supports the presence of allometry ($p = 0.0059$). In small lacrimals, the bone is T-shaped, and the anterior and posterior rami are shallow and horizontally oriented. The ventral ramus is gracile, and relatively tall (Fig. 5). In large lacrimals, the bone is 7-shaped, and the anterior ramus is deep and downturned. Additionally, the ventral ramus is broad, but its depth is relatively low in large lacrimals (Fig. 5).

The first two PCs explain about 83.7% of the total shape variation (PC1 = 48.3%, PC2 = 35.4%). In negative values of PC1, the bone is 7-shaped, due to

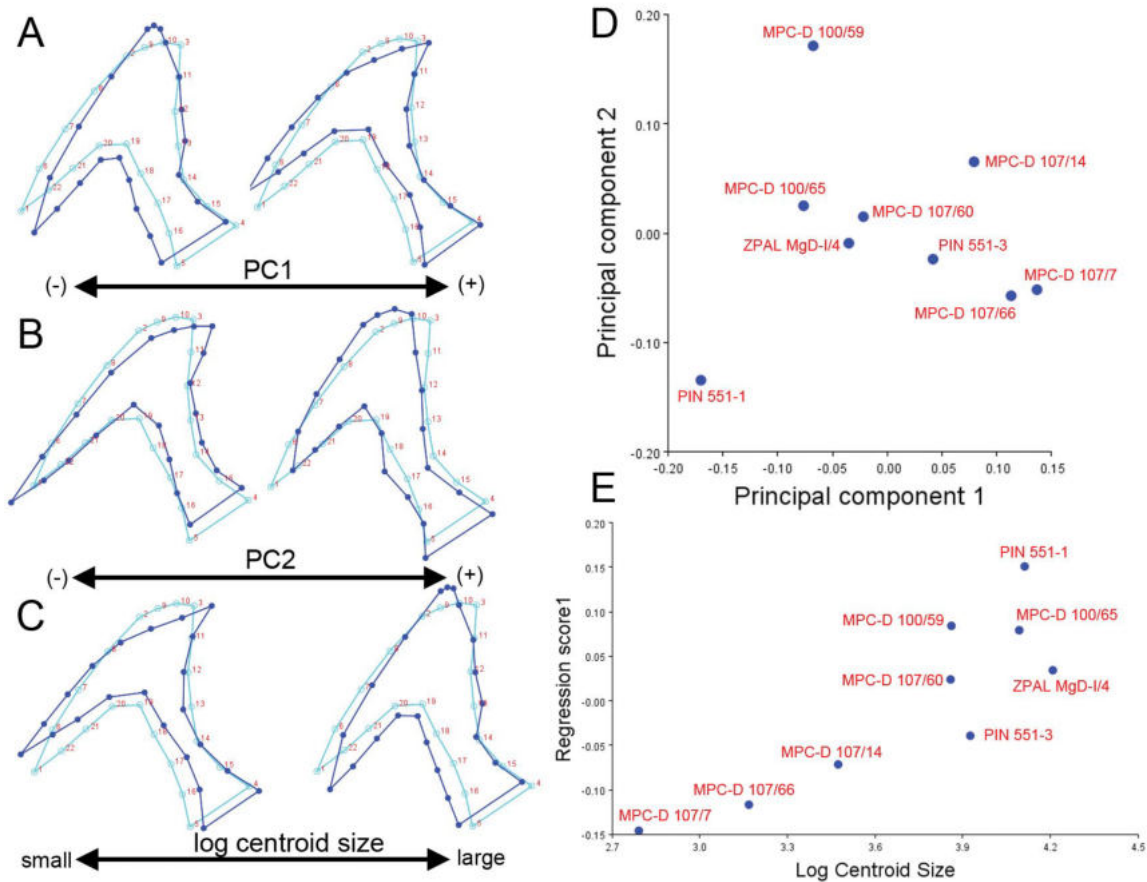


Fig. 5. *Tarbosaurus bataar* lacrimal shape analysed using geometric morphometrics. A, major changes in shape on PC1. B, major changes in shape on PC2. C, allometric analysis by multivariate regression of shape on log CS. D, two-dimensional morphospace defined by PC1 and PC2. E, scatter plot of regression scores against log CS. Red numbers indicate landmarks and semi-landmarks positions. Light blue wireframes represent the mean of variation, and dark blue wireframes represent major shape variation.

dorsoventral inflation of the posterior ramus and the downturn of the anterior ramus. The overall shape of the bone is robust due to deepening of anterior and posterior rami, and the ventral ramus is thick, yet its relative height is slightly low. In positive values of PC1, the lacrimal is T-shaped, mainly because the posterior ramus is dorsoventrally shallow and pointed, and the anterior ramus is horizontal. Additionally, the anterior, posterior and ventral rami are gracile, and this is most pronounced at the mid-height of the ventral ramus. Collectively, PC1 mostly describes the relative convexity of the posterior ramus, and the orientation of the anterior ramus (Fig. 5). In negative values of PC2, the bone is T-shaped, and the anterior ramus is shallow but elongate. The ventral ramus is slightly curved posteriorly, and it is relatively low. In positive values of PC2, the bone is 7-shaped, and the anterior ramus is deep but relatively short anteroposteriorly. The ventral ramus curves anteriorly, and it is relatively tall. The most significant variation described by PC2

appears to be the relative length of the anterior ramus (Fig. 5).

The regression analysis of the PC1 score against the log CS shows around 71.3% of PC1 is explained by the size, and this is statistically significant ($p = 0.0023$). In contrast, less than 1.3% of PC2 is found to be explained by size, but this is not significant statistically ($p = 0.7612$). Indeed, within the PC1 versus PC2 morphospace, larger lacrimals tend to have low PC1 values (Fig. 5).

Jugal

The regression of Procrustes coordinates onto log CS for *Tarbosaurus bataar* jugals indicates that 27.1% of the variation is explained by size ($n = 8$). Given that a correlation between shape and size is found to be significant ($p = 0.0262$), it is clear that allometric growth was present in the jugal of *Tarbosaurus bataar*. In small jugals, the main axis of the bone is

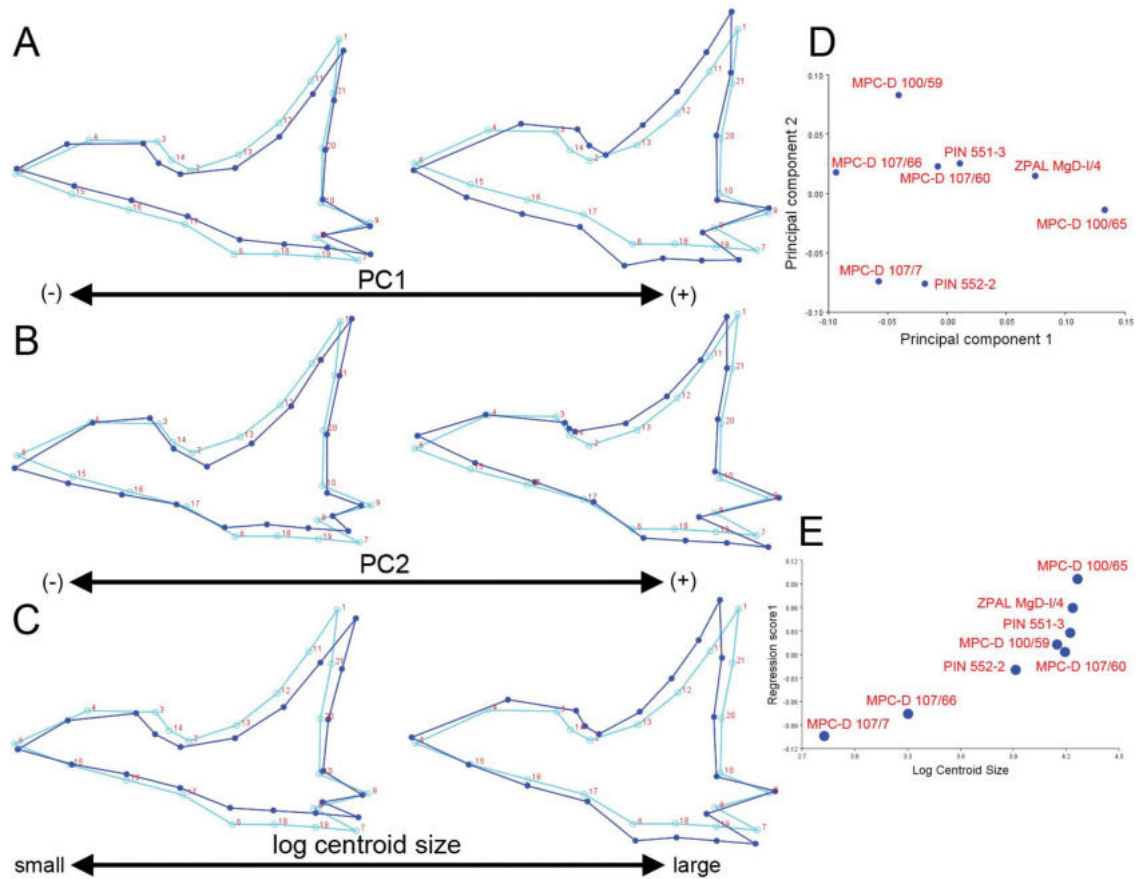


Fig. 6. *Tarbosaurus bataar* jugal shape analysed using geometric morphometrics. A, major changes in shape on PC1. B, major changes in shape on PC2. C, allometric analysis by multivariate regression of shape on log CS. D, two-dimensional morphospace defined by PC1 and PC2. E, scatter plot of regression scores against log CS. Red numbers indicate landmarks and semi-landmarks positions. Light blue wireframes represent the mean of variation, and dark blue wireframes represent major shape variation.

relatively horizontal. Additionally, the bone is relatively shallow, and the maxillary ramus is short. Furthermore, the lacrimal facet (line between landmarks 3 and 4; Fig. 1, Supplementary Online Material 2) is anteroventrally positioned, and the ventral margin of the orbit is elongate. The ascending ramus is inclined posteriorly, and it appears to be relatively slender. Lastly, the ventral flange of the jugal is underdeveloped, and the quadratojugal facet is dorsoventrally shallow (Fig. 6). In large jugals, the main axis of the bone slopes posteroventrally; the bone is dorsoventrally deep; and its maxillary ramus is elongate. The lacrimal facet is posterodorsally inclined, and the part that forms the ventral margin of the orbit is short. The ascending ramus is tall, vertically oriented and anteroposteriorly broad. Lastly, the ventral flange is well-developed, and the quadratojugal facet is dorsoventrally deep (Fig. 6).

The first two PCs explain about 62.0% of the total variation (PC1 = 40.4%, PC2 = 21.6%). Negative values of PC1 describe the relatively shallow body of the bone; short and shallow maxillary ramus; the elongate lacrimal facet that slopes anteroventrally; the elongate ventral margin of the orbit; relatively low and slender ascending ramus; and underdeveloped ventral flange of the jugal. Positive values of PC1 describe the dorsoventrally deep body of the bone; deep and elongate maxillary ramus; short lacrimal facet that is nearly horizontal; short ventral margin of the orbit; tall and broad ascending ramus; and well-developed ventral flange of the jugal. Collectively, the variation described by PC1 is mostly associated with the relative position of the lacrimal facet, the height of the ascending process and the depth of the bone (Fig. 6). Negative values of PC2 describe the deep maxillary ramus that is inclined anteroventrally; short lacrimal

facet; shallow suborbital region; elongate ventral margin of the orbit; anteroposteriorly short ascending ramus; and short, shallow facet for the quadratojugal. Positive values of PC2 describe the relatively shallow maxillary ramus that is inclined anteriorly; elongate lacrimal facet that is nearly horizontal; anteroposteriorly short ventral margin of the orbit; broad ascending ramus; and elongate and deep facet for the quadratojugal. Most of PC2 are associated with the relative length of the ventral part of the orbit, and the morphology of the quadratojugal facet (Fig. 6).

The regression analysis of the PC1 score against the log CS shows 44.1% of this component is explained by the size, and statistically it is marginally significant ($p = 0.0621$). The regression of PC2 onto log CS suggests 26.5% of PC2 is explained by the size, but this result is not significant ($p = 0.2042$). Certainly, there is a tendency for large jugals to have higher PC1 values (Fig. 6).

Postorbital

The regression of Procrustes coordinates onto log CS for *Tarbosaurus bataar* postorbitals indicates that 46.8% of the variation is explained by the size ($n = 8$), and this relationship is statistically significant ($p = 0.0048$). In small postorbitals, the anterior ramus is dorsoventrally shallow and anterodorsally inclined; the cornual process is underdeveloped; the ventral ramus is anteroposteriorly short, and its suborbital process is underdeveloped and ventrally positioned. This morphology results in a relatively large orbit in such small specimens. Finally, the posterior ramus is shallow, horizontal and posteriorly elongate (Fig. 7). In large postorbitals, the anterior ramus is deep and ventrally inclined, and its cornual process is tall and subcircular. Additionally, the ventral ramus is broad, and its suborbital process is well-developed and is positioned dorsally. This results in a relatively anteroposteriorly short orbit in large specimens. Lastly, the

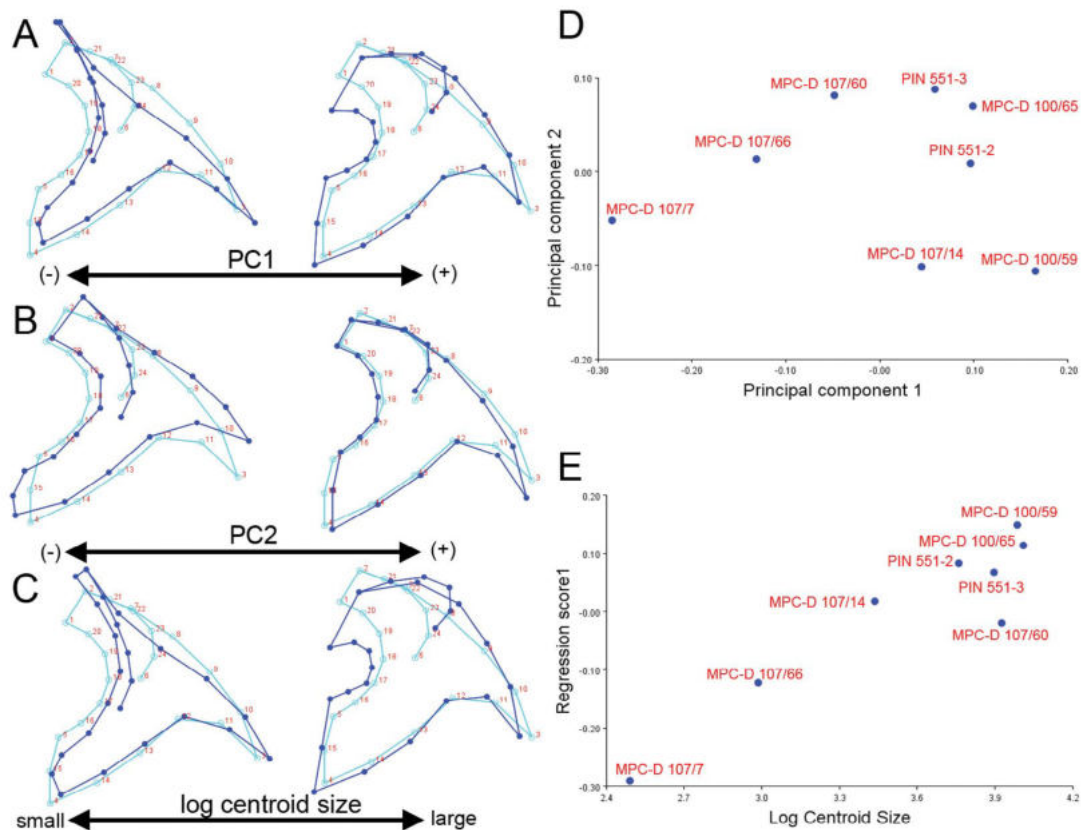


Fig. 7. *Tarbosaurus bataar* postorbital shape analysed using geometric morphometrics. A, major changes in shape on PC1. B, major changes in shape on PC2. C, allometric analysis by multivariate regression of shape on log CS. D, Two-dimensional morphospace defined by PC1 and PC2; E, the scatter plot of regression scores against log CS. Red numbers indicate landmarks and semi-landmarks positions. Light blue wireframes represent the mean of variation, and dark blue wireframes represent major shape variation.

posterior ramus is deep, but it is short and slopes ventrally (Fig. 7).

The first two PCs explain approximately 71.7% of the total variation (PC1 = 55.8%, PC2 = 15.9%). Negative values of PC1 describe a shallow anterior ramus with an underdeveloped cornual process; large orbit; slender ventral ramus with underdeveloped suborbital process; and shallow yet elongate posterior ramus. Positive values of PC1 describe a deep anterior ramus with well-developed, subcircular cornual process; anteroposteriorly narrow orbit; broad ventral ramus with well-developed suborbital process; and deep but short posterior ramus that curves ventrally. Collectively, PC1 mostly describes the variation in the relative size of the cornual process as well as the shape of the anterior ramus (Fig. 7). Negative values of PC2 describe a deep, dorsally inclined anterior ramus; shallow cornual process; anteroposteriorly short, anteriorly inclined ventral ramus with a small,

ventrally located suborbital process; and short posterior ramus that is inclined dorsally. Positive values of PC2 describe a shallow anterior ramus with subcircular cornual process, vertically inclined ventral ramus with dorsally located suborbital process, and an anteroposteriorly short posterior ramus that slopes ventrally. The most significant variation described by PC2 appears to be related to how much the posterior ramus curves downward (Fig. 7).

The regression analysis of the PC1 score against the log CS shows about 79.2% of PC1 is explained by the size of the bone, and this relationship is statistically significant ($p = 0.0074\%$). In contrast, size explains about 12.3% of the variation represented by PC2, and this relationship lacks statistical significance ($p = 0.4137$). Indeed, large postorbitals are distributed within the greater PC1 region of the morphospace (Fig. 7).

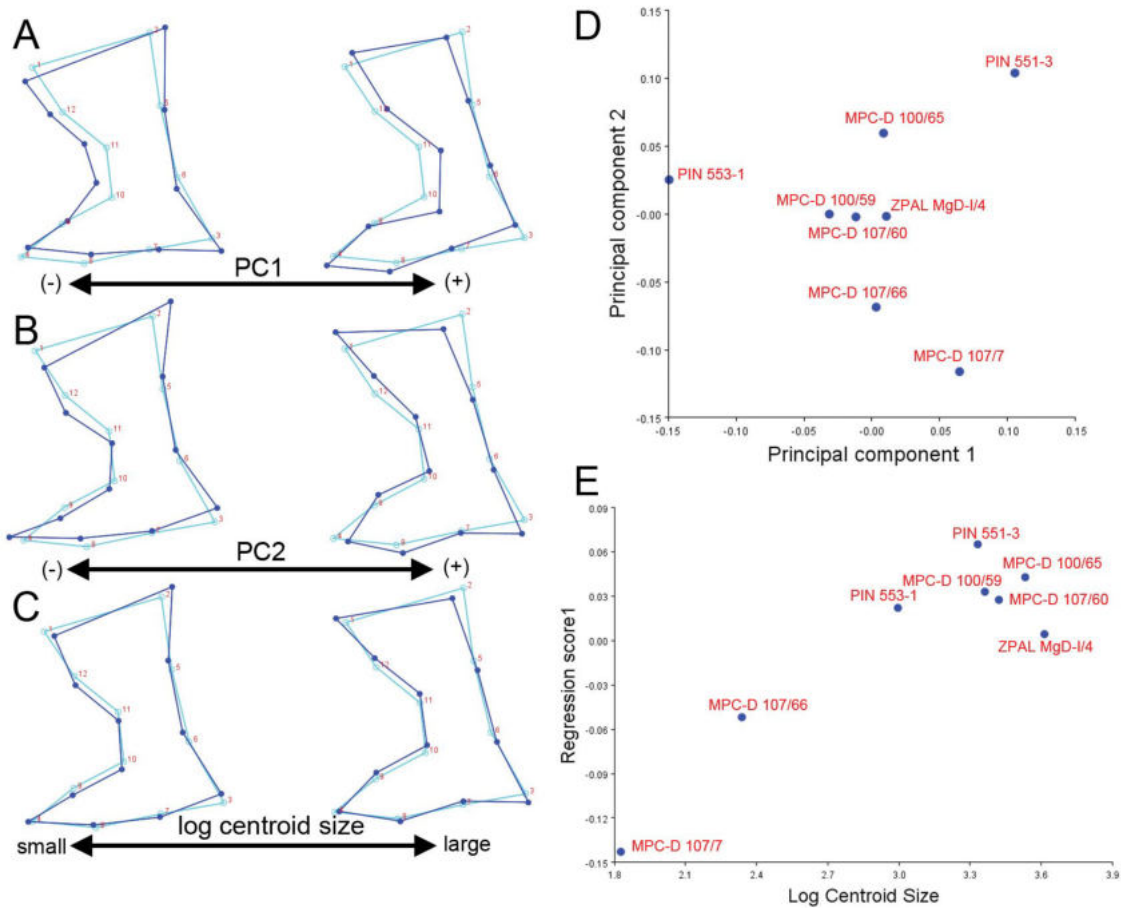


Fig. 8. *Tarbosaurus bataar* quadratojugal shape analysed using geometric morphometrics. A, major changes in shape on PC1. B, major changes in shape on PC2. C, allometric analysis by multivariate regression of shape on log CS. D, two-dimensional morphospace defined by PC1 and PC2. E, scatter plot of regression scores against log CS. Red numbers indicate landmarks and semi-landmarks positions. Light blue wireframes represent the mean of variation, and dark blue wireframes represent major shape variation.

Quadratojugal

The regression of Procrustes coordinates against log CS suggests 23.4% of the variation of *Tarbosaurus bataar* quadratojugals can be explained by size ($n = 8$). In small quadratojugals, the squamosal facet slopes posterodorsally, the anterior process is shallow, and the jaw joint is inclined dorsally (Fig. 8). In large quadratojugals, the squamosal facet slopes anterodorsally, and the anterior process is dorsoventrally deep. Finally, the jaw joint has shifted ventrally (Fig. 8). However, the correlation between the shape and size for the quadratojugal is found to have a weak statistical support ($p = 0.1006$).

The first two PCs explain about 65.5% of the total variation (PC1 = 35.4%, PC2 = 30.1%). Negative values of PC1 describe a broad squamosal facet that slopes posterodorsally; an anteroposteriorly long midheight of the vertical process; a shallow, short anterior process that is slightly inclined dorsally; and a jaw joint that has shifted posteroventrally. Positive values of PC1 describe an anteroposteriorly short squamosal facet that slopes anterodorsally; a short midheight region of the bone; a deep and elongate anterior process that is inclined anteroventrally; and a dorsally shifted jaw joint. Together, PC1 mostly describes a relative thickness of the midheight region and the depth of the anterior process (Fig. 8). Negative values of PC2 describe a broad squamosal facet that strongly slopes posterodorsally; a shallow, elongate anterior process in which its tip is slightly inclined dorsally; and a dorsally positioned jaw joint. Positive values of PC2 describe an anteroposteriorly short squamosal facet that slopes anterodorsally; a deep anterior process in which its tip is slightly inclined ventrally; and ventrally positioned jaw joint. Collectively, PC2 is mostly associated with the shape of the squamosal facet (Fig. 8).

The regression analysis of the PC1 score against the log CS suggests only about 2.0% of PC1 is explained by the size, and this relationship is not statistically significant ($p = 0.6873$). In contrast, size explains more than 63.4% of the variation described by PC2, and the correlation between them is statistically significant ($p = 0.0177$). Certainly, small quadratojugals are differentiated from the larger ones at negative PC2 values (Fig. 8).

Frontal

The regression of Procrustes coordinates against the log CS for *Tarbosaurus bataar* frontals indicates that around 81.9% of total shape variation can be accounted for by allometry ($n = 5$). In small frontals,

the body of the bone is triangular, and is anteroposteriorly elongate but mediolaterally narrow. Additionally, the nasal process is mediolaterally wide; the prefrontolacrimal process is short and inclined laterally; the lacrimal socket is elongate but mediolaterally narrow; the orbital slot is long; the width between the lateral edge of the postorbital buttress and the midline is significantly narrower compared to that between the most lateral point of the posterior shelf and the midline; and the dorsotemporal fossa is short and inclined anterolaterally (Fig. 9). In large frontals, the overall body of the bone is rectangular, and is broad but relatively short. Additionally, the nasal process is mediolaterally narrow; the prefrontolacrimal process is mediolaterally wide and inclined medially; the lacrimal socket is short but mediolaterally wide; the orbital slot is short; the width between the lateral edge of the postorbital buttress and the midline is nearly equal to that between the most lateral point of the posterior shelf and the midline; and the dorsotemporal fossa is broad, and its anterior margin is oriented mediolaterally (Fig. 9). The correlation between the size and shape is found to be significant ($p = 0.0096$).

The first two PCs account for about 94.9% of the total variation (PC1 = 90.0%, PC2 = 4.9%). Negative values of PC1 describe a mediolaterally narrow but anteroposteriorly elongate, triangular body of the bone; a mediolaterally broad nasal process; a short, triangular prefrontolacrimal process that is inclined laterally; an anteroposteriorly elongate but mediolaterally narrow lacrimal socket; an elongate orbital slot; a width between the lateral edge of the postorbital buttress and the midline that is significantly narrower compared to that between the most lateral point of the posterior shelf and the midline; and a short dorsotemporal fossa in which the anterior margin is inclined anterolaterally. Positive values of PC1 describe a broad but short, rectangular body of the bone; a mediolaterally narrow nasal process; a mediolaterally wide, triangular prefrontolacrimal process that is inclined medially; a short but mediolaterally wide lacrimal socket; a width between the lateral edge of the postorbital buttress and the midline that is nearly equal to that between the most lateral point of the posterior shelf and the midline; a short orbital slot; and a broad dorsotemporal fossa in which its anterior margin extends mediolaterally. Together, PC1 mostly describes the relative length and width of the bone, and the broadness of the dorsotemporal fossa (Fig. 9). Negative values of PC2 describe a broad nasal process; underdeveloped prefrontolacrimal process; a short but mediolaterally wide lacrimal socket in which the posterior margin is inclined anteromedially; a

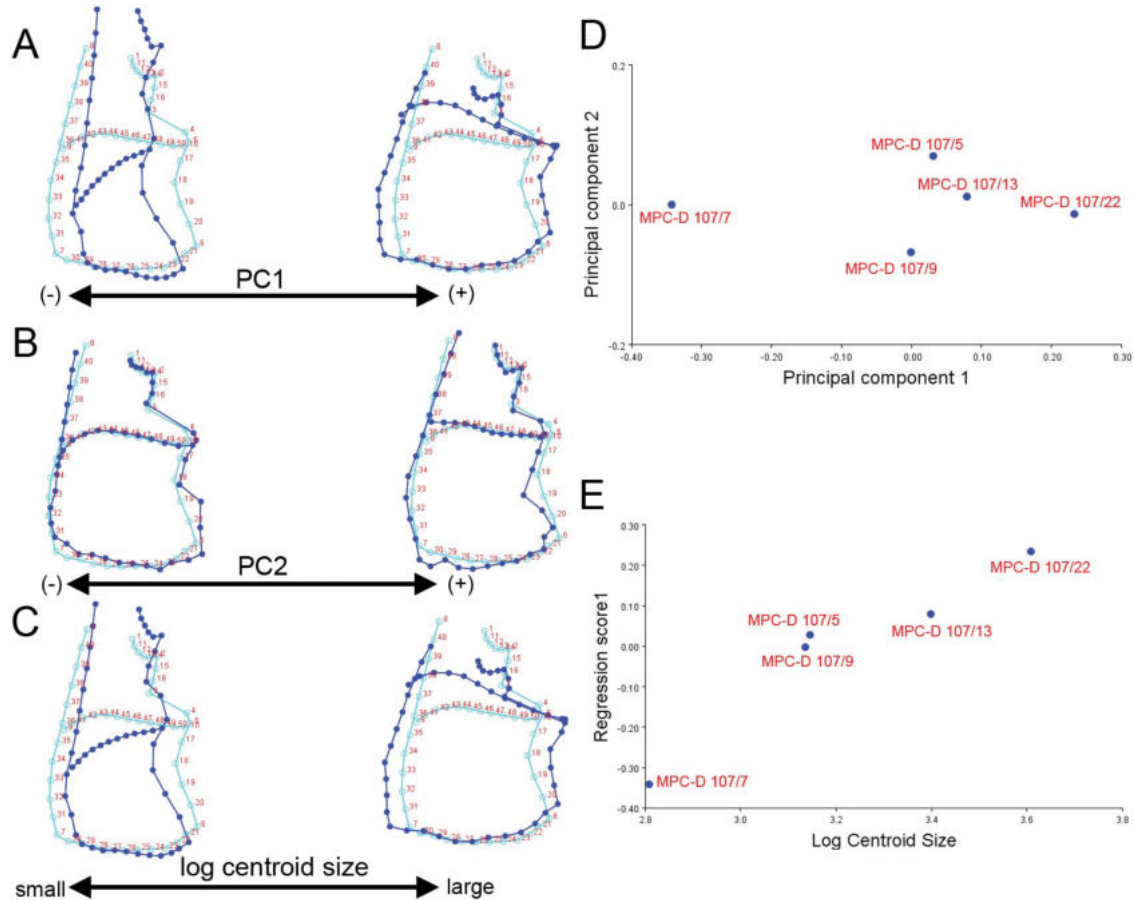


Fig. 9. *Tarbosaurus bataar* frontal shape analysed using geometric morphometrics. A, major changes in shape on PC1. B, major changes in shape on PC2. C, allometric analysis by multivariate regression of shape on log CS. D, two-dimensional morphospace defined by PC1 and PC2. E, scatter plot of regression scores against log CS. Red numbers indicate landmarks and semi-landmarks positions. Light blue wireframes represent the mean of variation, and dark blue wireframes represent major shape variation.

short orbital slot; an anteriorly positioned concavity at the area between the postorbital buttress and the posterior shelf; and a dorsotemporal fossa in which the medial part extends posteriorly. Positive values of PC2 describe a mediolaterally narrow nasal process; a mediolaterally narrow, triangular prefrontolacrimal process that is inclined anteriorly; a relatively long but narrow lacrimal socket; a relatively long orbital slot; a posteriorly positioned concavity at the area between the postorbital buttress and the posterior shelf; and a dorsotemporal fossa in which its anterior margin is nearly horizontal. Most of PC2 is associated with the shape of the medial part of the anterior margin of the dorsotemporal fossa, and the shape of the area between the postorbital buttress and the posterior shelf (Fig. 9).

Regression of PC1 against the log CS indicates that PC1 is significantly correlated with size ($p = 0.0099$), and more than 90.7% of PC1 can be explained by

allometry. In contrast, less than 0.2% of PC2 is found to be explained by size, and the correlation between them is insignificant ($p = 0.9926$). Unsurprisingly, within the PC1 versus PC2 morphospace, the smallest specimen in the sample (MPC-D 107/7) is differentiated from the larger specimens by its exceptionally low PC1 value (Fig. 9).

Parietal

The regression of Procrustes coordinates against the log CS for *Tarbosaurus bataar* parietals suggests 48.8% of the total shape variation can be accounted for by allometry ($n = 4$), and this correlation is statistically significant ($p = 0.0370$). In small parietals, the median spur is mediolaterally narrow and anteroposteriorly elongate; the sutural surface for the frontal is mediolaterally wide; the midlength region of the bone is thick; and the nuchal crest is anteroposteriorly

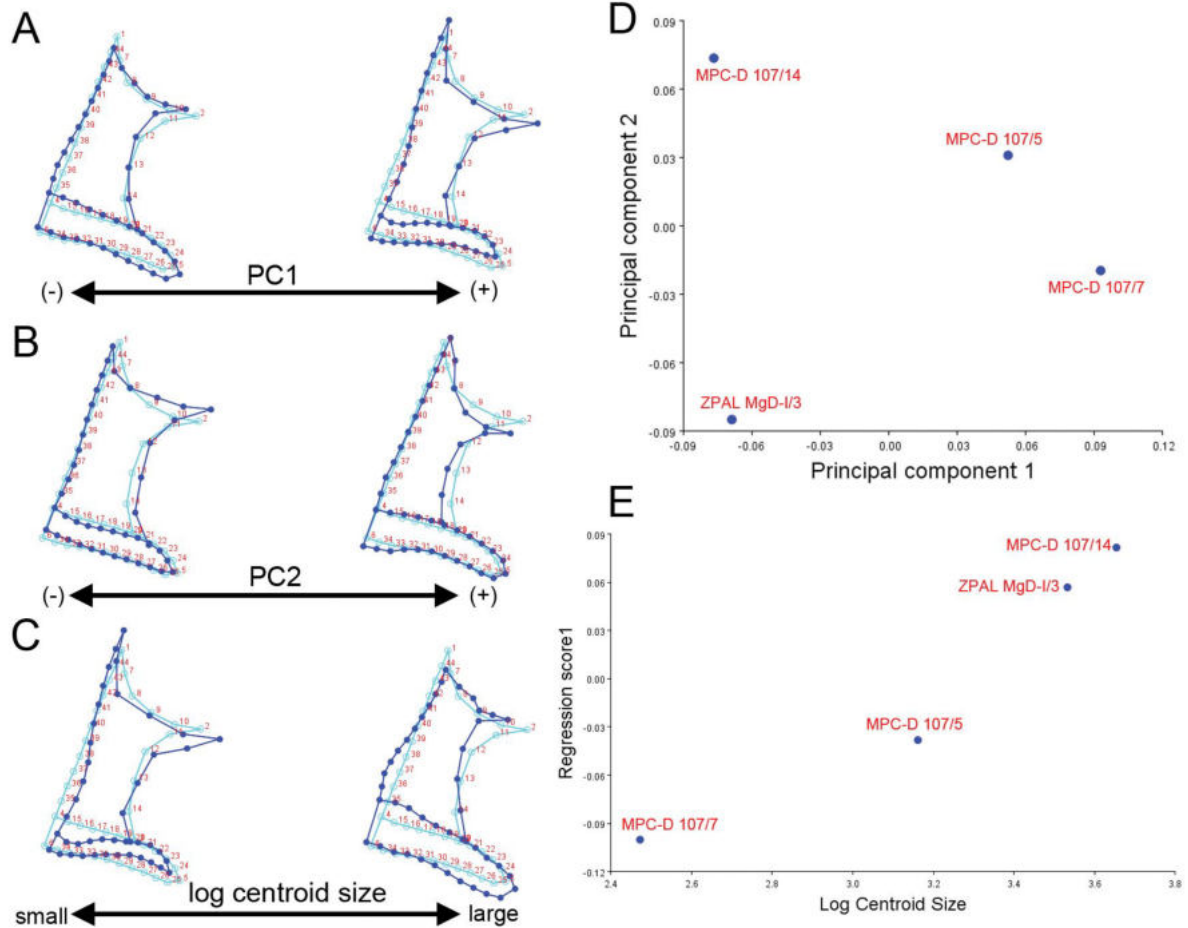


Fig. 10. *Tarbosaurus bataar* parietal shape analysed using geometric morphometrics. A, major changes in shape on PC1. B, major changes in shape on PC2. C, allometric analysis by multivariate regression of shape on log CS. D, two-dimensional morphospace defined by PC1 and PC2. E, the scatter plot of regression scores against log CS. Red numbers indicate landmarks and semi-landmarks positions. Light blue wireframes represent the mean of variation, and dark blue wireframes represent major shape variation.

thin, transversely narrow and inclined anterolaterally (Fig. 10). In large parietals, the median spur is thick but short; the sutural surface for the frontal is relatively narrow; the midlength region of the bone is mediolaterally narrow, and its lateral margin is strongly concave; and the nuchal crest is thick, mediolaterally wide and slightly inclined posterolaterally (Fig. 10).

The first two PCs explain about 87.5% of the total variation (PC1 = 53.5%, PC2 = 34.0%). Negative values of PC1 describe a broad but short median spur; relatively narrow sutural surface for the frontal; a transversely narrow midlength region of the bone with strongly concave lateral margin; and mediolaterally wide nuchal crest that is long anteroposteriorly. Positive values of PC1 describe a narrow, anteroposteriorly elongate median spur; a relatively wide sutural surface for the frontal; broad midlength region of the

bone with weakly concave lateral margin; and mediolaterally narrow nuchal crest that is anteroposteriorly thin. Collectively, the variations described by PC1 are mostly associated with the width and anteroposterior length of the nuchal crest, and the width of the midlength region of the bone (Fig. 10). Negative values of PC2 describe a broad and elongate median spur; posterolaterally oriented sutural surface for the frontal; mediolaterally narrow midlength region of the bone in which two-thirds of the lateral margin is nearly straight; and a nuchal crest that is slightly inclined posteromedially. Positive values of PC2 describe a short and narrow median spur; mediolaterally oriented sutural surface for the frontal; mediolaterally broad midlength region of the bone; and a nuchal crest in which its medial part is inclined anteriorly. Collectively, PC2 mostly describes the relative

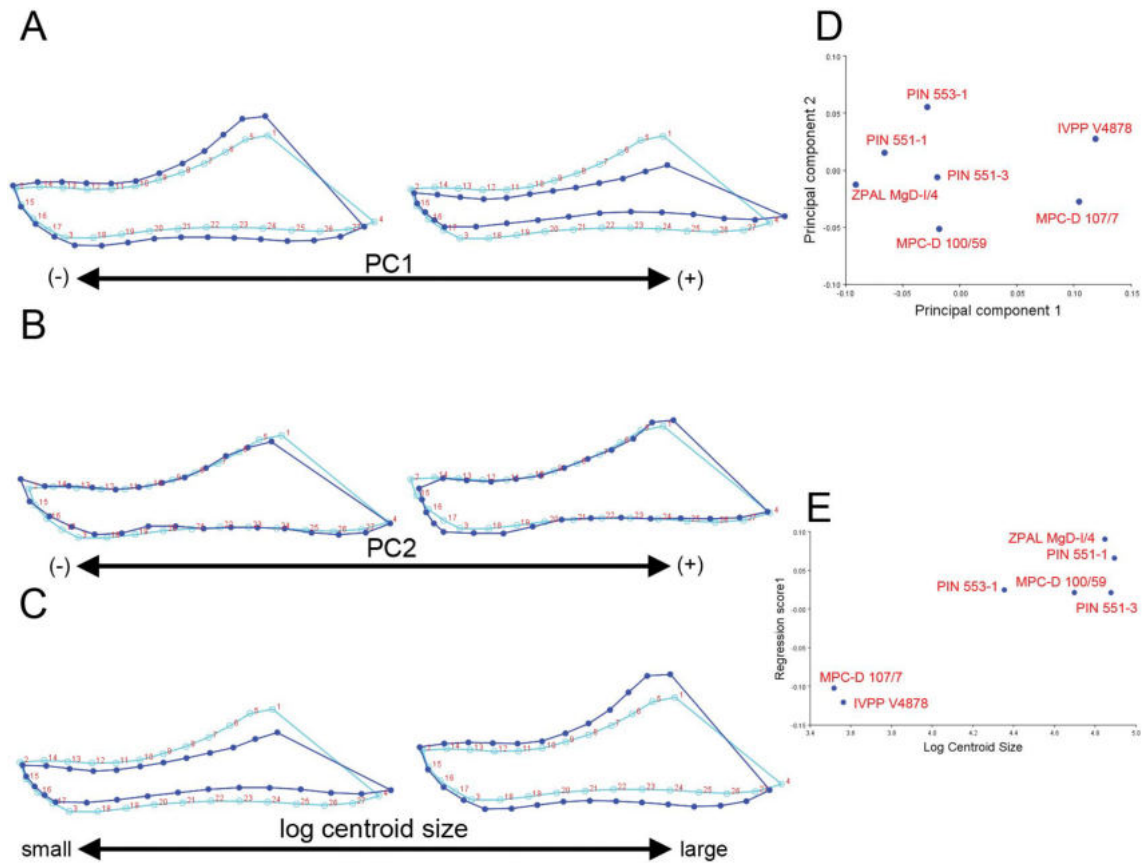


Fig. 11. *Tarbosaurus bataar* dentary shape analysed using geometric morphometrics. A, major changes in shape on PC1. B, major changes in shape on PC2. C, allometric analysis by multivariate regression of shape on log CS. D, two-dimensional morphospace defined by PC1 and PC2. E, the scatter plot of regression scores against log CS. Red numbers indicate landmarks and semi-landmarks positions. Light blue wireframes represent the mean of variation, and dark blue wireframes represent major shape variation.

length of the median spur, and the orientation of the sutural surface for the frontal (Fig. 10).

The regression of PC1 against the log CS suggests approximately 87.0% of PC1 is explained by size, and this correlation is statistically significant ($p = 0.0411$). In contrast, only about 2.8% of PC2 can be accounted for by allometry, and the relationship between PC2 and size is not statistically significant ($p = 0.7541$). Indeed, large specimens have lower PC1 values, whereas small parietals exhibit high PC1 scores (Fig. 10).

Dentary

The regression of Procrustes coordinates against the log CS for *Tarbosaurus bataar* dentaries suggests approximately 69.4% of the total shape variation can be accounted for by allometry ($n = 7$). In small dentaries, the overall body of the bone is shallow; the

anterior margin is short, weakly convex and slopes posteroventrally; there is an anteriorly positioned inflection point ('chin') where anterior and ventral margins meet; the alveolar margin is weakly concave; the ventral margin is weakly sigmoidal; and the posterior region is elongate but shallow (Fig. 11). In large dentaries, the bone is dorsoventrally deep; the anterior margin is convex, elongate and slopes posteroventrally; the inflection point is more posterior; the alveolar margin is deeply concave; the ventral margin is sigmoidal; and the posterior region is short but dorsoventrally deep (Fig. 11). The correlation between the shape and size is statistically significant ($p = 0.0127$).

The first two PCs account for about 93.5% of the total shape variation (PC1 = 78.2%, PC2 = 15.3%). Negative values of PC1 describe a dorsoventrally deep body of the bone; a deep, convex anterior margin that slopes posteroventrally; a posteriorly positioned inflection point; a strongly concave alveolar margin;

a sigmoidal ventral margin; and a dorsoventrally deep but anteroposteriorly short posterior region of the bone. Positive values of PC1 describe a dorsoventrally shallow body of the bone; a shallow, weakly convex anterior margin that slopes posteroventrally; an anteriorly positioned inflection point; a weakly concave alveolar margin; a weakly sigmoidal ventral margin; and an elongate but shallow posterior region. Together, PC1 mostly describes the variation in the relative depth of the bone, especially in the posterior region (Fig. 11). Negative values of PC2 describe a relatively shallow body of the bone; a convex anterior margin that strongly slopes posteroventrally; a concave alveolar margin in which the anterior part slopes anterodorsally; a posteriorly positioned inflection point; a sigmoidal ventral margin; and relatively long but shallow posterior region. Positive values of PC2 describe the relatively deep body of the bone; a weakly convex anterior margin that is oriented subvertically; a concave alveolar margin in which the anterior part

slopes anteroventrally; an anteriorly positioned inflection point; a sigmoidal ventral margin; and a relatively deep but short posterior region. The majority of PC2 is related to the shape of the anterior part of the alveolar margin, and the orientation of the anterior margin of the bone (Fig. 11).

The regression of PC1 against log CS suggests more than 88.2% of PC1 is explained by size, and this correlation is significant ($p = 0.0123$). In contrast, no significant relationship is found between PC2 and log CS ($p = 0.7563$), and allometry accounts for less than 1.8% of this principal component. Certainly, large dentaries are clustered in the negative PC1 region within the PC1 versus PC2 morphospace (Fig. 11).

Surangular

The regression of Procrustes coordinates against the log CS for surangular bones of *Tarbosaurus bataar* suggests about 23.5% of the variation is explained by

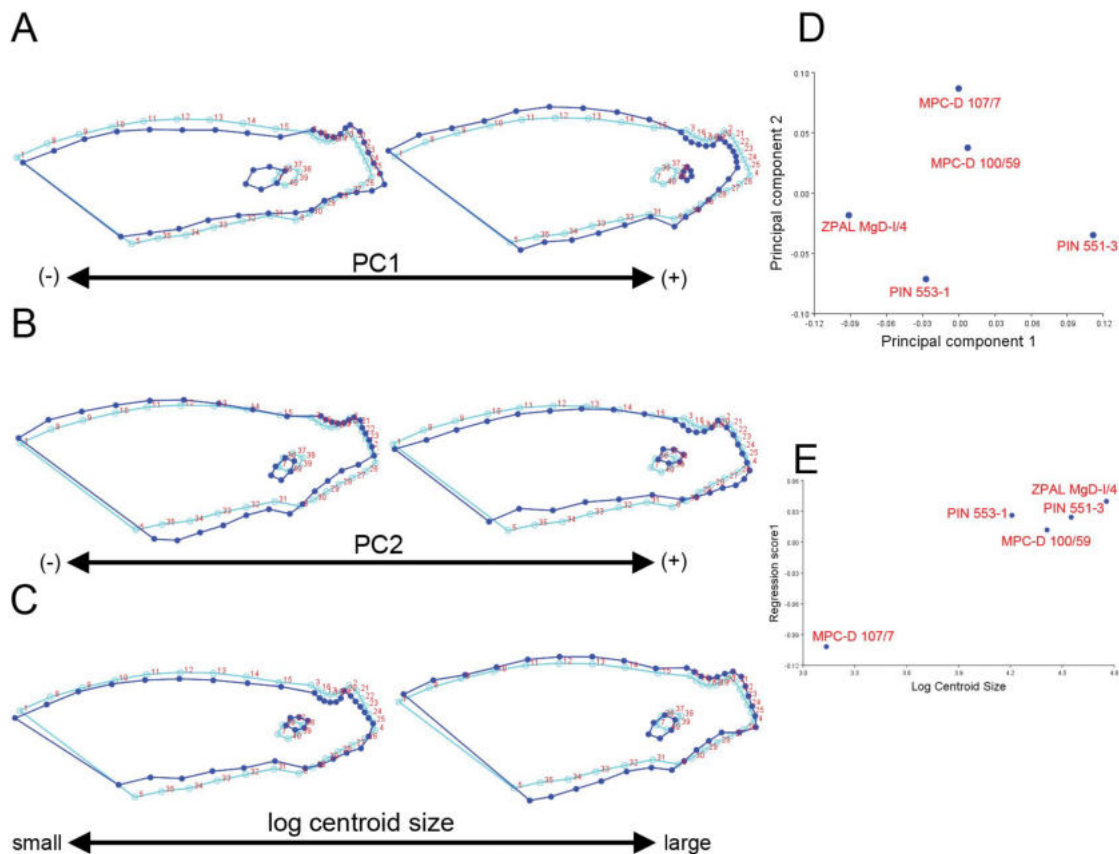


Fig. 12. *Tarbosaurus bataar* surangular shape analysed using geometric morphometrics. A, major changes in shape on PC1. B, major changes in shape on PC2. C, allometric analysis by multivariate regression of shape on log CS. D, two-dimensional morphospace defined by PC1 and PC2. E, scatter plot of regression scores against log CS. Red numbers indicate landmarks and semi-landmarks positions. Light blue wireframes represent the mean of variation, and dark blue wireframes represent major shape variation.

size ($n = 5$), but this correlation is not statistically significant ($p = 0.5806$). In small surangulars, the bone is dorsoventrally shallow; the dorsal margin is gently convex; the glenoid is short and deep; the posterior margin of the retroarticular process is shallow and slopes posteroventrally; the posteroventral margin is short and weakly convex; the ventral margin is horizontal; and the surangular foramen is small and posterodorsal in position (Fig. 12). In large surangulars, the bone is dorsoventrally deep; the dorsal margin is convex; the glenoid is elongate and relatively shallow; the posterior margin of the retroarticular process is deep and subvertical; the posteroventral margin is concave; the ventral margin is relatively short and slopes anteroventrally; and the surangular foramen is slightly enlarged and more anteroventral in position compared to small individuals (Fig. 12).

The first two PCs explain approximately 69.9% of the total shape variation (PC1 = 40.6%, PC2 = 29.3%). In negative values of PC1, the bone is dorsoventrally shallow; the dorsal margin is weakly convex; the glenoid is deeply concave; the posterior margin of the retroarticular process is deep and relatively straight; the posteroventral margin is shallow, weakly concave and horizontal; the ventral margin is relatively straight; and the surangular foramen is enlarged and is positioned anteriorly. In positive values of PC1, the bone is dorsoventrally deep; the dorsal margin is strongly convex; the glenoid is shallowly concave; the posterior margin of the retroarticular process is shallow and convex; the posteroventral margin is deep and slopes anteroventrally; the ventral margin is concave and slopes anteroventrally; and the posterior surangular foramen is diminutive and is posterior in position. The most significant variation described by PC1 appears to be related to relative position and the size of the posterior surangular foramen (Fig. 12). In negative values of PC2, the bone is dorsoventrally deep; the dorsal margin is convex; the glenoid is short and weakly concave; the posterior margin of the retroarticular process is relatively shallow and straight; the posteroventral margin is relatively long and slopes anteroventrally; the ventral margin is short, concave and slopes anteroventrally; and the posterior surangular foramen is located anteroventrally relative to the posterior margin of the bone. In positive values of PC2, the bone is dorsoventrally shallow; the dorsal margin is gently convex; the glenoid is elongate and concave; the posterior margin of the retroarticular process is deep and weakly convex; the posteroventral margin is short and slopes weakly anteroventrally; the ventral margin is elongate and nearly horizontal; and the posterior surangular foramen is positioned

more posterodorsally. The most significant variation described by PC2 appears to be related to the orientation of the ventral margin (Fig. 12).

The regression of PC1 against log CS suggests less than 0.3% of PC1 is explained by size, and this correlation is not statistically significant ($p = 0.9272$). The regression of PC2 onto log CS indicates more than 46.0% of this PC can be explained by size, and even though it is also not significant, it has a slightly higher statistical power than the case of PC1 ($p = 0.1928$). Indeed, there seems to be a tendency for large specimens to have lower PC2 scores (Fig. 12).

Discussion

Allometric shape change in individual elements

Analyses of various craniomandibular bones of *Tarbosaurus bataar* reveal that major allometric shape changes include dorsoventral deepening of maxilla, nasal, jugal and dentary; the transition from a T-shape to a 7-shape of the lacrimal (most likely due to inflation of the posterior ramus; e.g. Hurum & Sabath 2003; Tsuihiji *et al.* 2011); anteroposterior relative shortening of the orbit (=transitioning from oval to keyhole-shape) accompanied by broadening of the postorbital as well as the development of the suborbital process of the bone; enlargement of the cornual processes of the postorbital and the ventral flange of the jugal; widening and relative shortening of the frontal accompanied by a broadening of the dorsotemporal fossa; and widening and thickening of the nuchal crest accompanied by the narrowing of the midlength region of the parietal. Although three of the examined parts (premaxilla, quadratojugal, surangular) are found to be not statistically different from isometry, it is possible that these cases represent instances of 'soft isometry' that is imposed by small sample size or the nature of the dataset that is heavily skewed to relatively large specimens (Brown & Vavrek 2015), or the result of two-dimensional simplification of three-dimensional bones. According to Carr (2020), elements like the premaxilla, quadratojugal or surangular went through relatively small numbers of changes during growth compared to many other craniomandibular bones (maxilla frontal, dentary) in *Tyrannosaurus rex*. Given that *Tarbosaurus bataar* and *Tyrannosaurus rex* are closely related, it is reasonable to assume that general trends in growth were largely similar as well (Carr 2020). If this is the case, this may be the reason why no significant allometric growth pattern was observed in these elements compared to other craniomandibular bones in this work.

Indeed, although not being statistically significant, the allometric shape change trends observed in these bones, such as the increase of height accompanied by a posterodorsal shift of the external naris in the premaxilla; concealment (narrowing) of the maxillary process in lateral view of the premaxilla; shortening of the premaxilla in lateral view that is assumed to be the result of mediolateral widening and reorientation of the bone; increase of the depth of the surangular; and a posteroventral shift of the jaw joint of the quadratojugal are very similar to those observed in other tyrannosaurids (Carr 1999, 2020; Voris *et al.* 2022) or potentially other archosauriformes (Carr 2020). Thus, it is provisionally assumed that allometric growth changes were indeed present in these parts, although this assumption will need to be tested through reanalysis by including more specimens from a broader size range in the future.

Collectively, the major growth change patterns in craniomandibular bones of *Tarbosaurus bataar* are largely in accordance with those seen in North American tyrannosaurids (Carr 1999; Currie 2003a, b; Voris *et al.* 2019, 2022), particularly *Tyrannosaurus rex* as seen in the transformation of the lacrimal from a T-shape to 7-shape, an increase of the convexity of the alveolar margin of the maxilla, development of the subcircular cornual process of the postorbital, and the medial inclination of the prefrontolacrimal process of the frontal (Carr & Williamson 2004; Carr 2020). These results most likely reflect their close evolutionary relationship (Brusatte & Carr 2016; Carr *et al.* 2017) as well as great resemblance in external morphology (Hurum & Sabath 2003). Furthermore, it provides another quantitative support to prevailing orthodoxy that overall sequence of growth changes in craniofacial anatomy of tyrannosaurids is fairly conservative within this clade (Carr 1999, 2020; Currie 2003a, b; Carr & Williamson 2004; Voris *et al.* 2022). Finally, Tsuihiji *et al.* (2011) indicated *Tarbosaurus bataar* went through an ontogenetic trajectory that is similar to North American tyrannosaurids like *Tyrannosaurus rex*, although no quantitative evidence was provided. This hypothesis, however, is supported by our analyses, based on the expanded morphological dataset.

The vast majority of these changes are most likely related to a disproportionate increase of the bite forces during growth (e.g. Carr 2020). The increases of the heights of bones that compose the snout (maxilla, nasal, dentary) indicate an improvement of resistance to loads imposed by biting, tearing or growth-related increases in bite force (Carr & Williamson 2004; Rayfield 2004; Bates & Falkingham 2012; Brusatte & Carr 2016; Carr 2020; Rowe &

Snively 2022; Johnson-Ransom *et al.* 2024). Another indicator of enhanced bite forces are increases in the heights and widths of the teeth, which are extreme in *Tarbosaurus bataar* and *Tyrannosaurus rex* in that the basal widths of the crowns are nearly equal to the basal lengths (Currie & Azuma 2006; Brusatte & Carr 2016). Increase of depth is also seen in the jugal and the postorbital, which reflects an increase in height of the adductor region of the skull, indicating an expansion of the temporal musculature complex (Molnar 2013). Furthermore, these bones provide structural support of the postorbital region of the skull (e.g. Rayfield 2004; Sullivan & Xu 2017), and dorsoventral deepening and anteroposterior broadening of these bones would have made the skull mechanically stronger. Shape changes in the orbit, such as negative allometry in anteroposterior length and transition from oval to keyhole shape that are accompanied by allometric shape changes of the adjacent bones (lacrimal, postorbital, jugal), would have made the skull more beneficial in dissipating and mitigating feeding-induced stresses, and provide more cranial strength (Henderson 2002; Lautenschlager 2022). The changes are also correlated with the negative allometric growth of the eyeball and brain (Currie 2003b; Yun *et al.* 2022). Carr (2020) regarded ontogenetic transition from T-shape to 7-shape of the lacrimal in *Tyrannosaurus rex* was correlated with an increase of bite force of this taxon, and the shared growth trend in *Tarbosaurus bataar* is assumed to be related to the same phenomenon. The results of this work reaffirm those of Yun *et al.* (2022), who found allometric increases in the width of the frontal and the extension of dorsotemporal fossa onto it, and a negative allometry of the relative length of the frontal. The length of the brain scaled with negative allometry with the body size in tyrannosaurids (Currie 2003b), and given that the frontal length is strongly correlated with the size of the brain, it is no surprise that the length of this bone grows with negative allometry (Yun *et al.* 2022). Widening and expanding of the frontal and the dorsotemporal fossa, indicate the disproportionate increase of the jaw adductor musculature and its attachment area onto the skull roof as the animal grew (Carr 2020; Yun *et al.* 2022). In this study, the midlength region of the parietal was found to become proportionally narrower and its lateral edges become more concave as the animal size increased. Given that this area represents the medial part of the dorsotemporal fenestra, which was filled with an enormous volume of jaw adductor muscles in life (Gignac & Erickson 2017); the narrowing of the parietal midlength region is probably associated with the broadening of the dorsotemporal fenestra as the animals increased in size.

Based on these observations, it is probable that shared allometric growth trends in various craniomandibular bones (skull deepening, and increased robusticity) between *Tarbosaurus bataar*, and other tyrannosaurids like *Tyrannosaurus rex* are consequences of strengthening the skull structure in response to increased loads imposed by bite forces as well as the size increases of the adductor musculature during growth. Observed allometric shape change patterns suggest that in *Tarbosaurus bataar*, the relative depth of the surangular increased and the quadratojugal jaw joint angled downward during growth, similar to other tyrannosaurids (Carr 1999, 2020, Voris et al. 2022). However, given that these changes are statistically indistinguishable from isometry, such interpretation warrants caution.

The fact that some of the allometric shape change patterns of individual craniomandibular elements that are related to strengthening the skull structure in *Tarbosaurus bataar* (e.g. transition of the lacrimal from a T-shape to a 7-shape) are similar to *Tyrannosaurus rex* over other tyrannosaurids, indicates the cranium of mature individuals of this taxon was mechanically stronger than most other tyrannosaurids, and perhaps capable of generating higher bite forces. This is provisionally supported by greatly expanded width of the maxillary and dentary tooth crowns of this taxon, which is nearly equal to the basal length and shared with *Tyrannosaurus rex* (Samman et al. 2005; Currie & Azuma 2006; Brusatte & Carr 2016). Indeed, a study of Sakamoto (2022) showed that the bite force of *Tarbosaurus bataar* was significantly higher than other tyrannosaurids (*Daspletosaurus torosus*, *Gorgosaurus libratus*, *Teratophoneus curriei*), even if was not at the level of adult *Tyrannosaurus rex*. This may contradict the results of Johnson-Ransom et al. (2024), which found the bite force of an adult *Tarbosaurus bataar* is lower than that of smaller *Daspletosaurus torosus* in both relative and absolute terms. The adult *Tarbosaurus bataar* used in that work is based on ZPAL MgD-I/4, after Hurum & Sabath (2003; E. Johnson-Ransom, personal communication, 2023). However, the skull of ZPAL MgD-I/4 is too narrow as reconstructed in Hurum & Sabath (2003), and in reality, the cranium of *Tarbosaurus bataar* is as broad as in *Daspletosaurus torosus* (Currie 2003a; Hurum & Sabath 2003, fig. 15; Paul 2008; Loewen et al. 2013). This may have significantly affected the results of Johnson-Ransom et al. (2024), as it would have effects on mechanical strength of the snout, cross-sectional area of the adductor chamber, and consequently estimated jaw muscle forces. Indeed, bending strength analyses of theropod mandibles have found that the largest albertosaurines

and *Daspletosaurus torosus* were capable of generating similar bite forces with similar-sized *Tyrannosaurus rex* individuals (Therrien et al. 2005, 2021). Considering that the mandibular anatomy of *Tarbosaurus bataar* is largely similar to other tyrannosaurids (Hurum & Currie 2000; Currie 2003a; Hurum & Sabath 2003), it is expected that the dorsoventral bending force of the lower jaw (a valid proxy for a bite force; Therrien et al. 2005, 2021) of an adult *Tarbosaurus bataar* would be similar to equivalently-sized individual of *Tyrannosaurus rex*.

The relative size of the cornual process on the postorbital increased as the animals grew. Unless there is compelling counter-evidence, such as cranial ornamentations in non-avian dinosaurs, including theropods, are best interpreted as socio-sexual display structures (Hone et al. 2012). It is recognized that the general growth patterns of many sexually selected traits have positive allometry; the fact that cranial ornamentations in at least some dinosaurs had such growth patterns have been suggested as evidence that they likely evolved as a result of pressures favoring socio-sexual display signals (Gates et al. 2016; Hone et al. 2016; Knapp et al. 2021). The positive allometry in cornual processes in the postorbital in *Tarbosaurus bataar* may imply cranial ornamentations in this taxon, and other tyrannosaurids (for example, see Brusatte & Carr 2016), were primarily used for socio-sexual display. Indeed, relative increases of the sizes of cornual processes in craniofacial bones such as the postorbital during growth (=positive allometry) is observed in other tyrannosaurids as well (Voris et al. 2019).

According to Sharpe et al. (2025), the ventral flange of tyrannosaurid jugal, which is often termed as the ‘cornual process’ or ‘jugal horn’ (Carr et al. 2017; Coppock et al. 2024) and interpreted as a horn-like, cranial display feature in previous literature (Sullivan & Xu 2017; Carr et al. 2017), actually represents a ventral part of an attachment area for the ‘exoparia’ muscle or ligament connecting the zygoma and the mandible. The positive allometry in the ventral flange of the jugal in *Tarbosaurus bataar* observed in this work, would be consistent with a relatively large ‘exoparia’ soft tissue in large individuals. Considering that a connective tissue bridging the zygoma and the mandible would be helpful to stabilize the mandible during jaw movement (Sharpe et al. 2025), a proportionally large ‘exoparia’ in large individuals may have been helpful to endure high loadings during powerful bite, feeding and hunting. Such observation is potentially corroborated by an ontogeny of the lateral rugosity of the jugal: a lateral rugosity of the jugal, which extends anterodorsally from the ventral flange, most

likely represents an anterolateral attachment area of the 'exoparia' (Sharpe *et al.* 2025). Intriguingly, in immature tyrannosaurid individuals, including those of *Tarbosaurus bataar* (Tsuihiji *et al.* 2011, fig. 8), such rugosities are largely underdeveloped or absent, unlike the adults with highly rugose nature of this region (Brusatte *et al.* 2012a; Voris *et al.* 2022, fig. 6; Coppock *et al.* 2024, fig. 5).

Results of this work suggest allometric increases in the width and anteroposterior thickness of the nuchal crest of the parietal in *Tarbosaurus bataar*. Tsuihiji *et al.* (2011) also noted an ontogenetic increase of the height of the crest in *Tarbosaurus*. Similar trends have been noted for North American tyrannosaurids as well (Carr 1999; Voris *et al.* 2022). Considering that the nuchal crest served as an attachment area for the cranial dorsoflexor neck muscles, it is probable that changes in this area are related to shifts in strength, mobility of the neck musculature or feeding behavior (Snively & Russell 2007; Tsuihiji 2010; Voris *et al.* 2022). Note, however, that our sample size of the parietal is small ($N = 4$), and therefore the observed allometric growth pattern for this element ideally should have a larger sample size in subsequent studies.

Ontogenetic allometry of Tarbosaurus bataar craniomandibular bones in comparison with other tyrannosaurids

The results of this work suggest the main shape change patterns in craniomandibular anatomy of *Tarbosaurus bataar* are broadly congruent with those of other tyrannosaurids. However, at least some of the observed modifications deserve some further discussion as they appear to be unique to this taxon. These are characters that were unrecognized in previous works (Tsuihiji *et al.* 2011; Yun *et al.* 2022) that addressed the ontogeny of *Tarbosaurus bataar* or bear some implications about our current knowledge about growth in tyrannosaurids. In their extensive description about craniofacial ontogeny of *Gorgosaurus libratus*, Voris *et al.* (2022) noted the substantial dorsoventral expansion of the posterior region of the dentary during growth, and regarded this as a unique feature of this taxon. However, it appears that as the animals increased in size, the posterior region of the dentary in *Tarbosaurus bataar* deepened to the extent that is comparable to, or perhaps even more than what is observed in *Gorgosaurus libratus* (Voris *et al.* 2022, fig. 9). All tyrannosaurids had an allometric increase in the depth of the dentary in mature individuals (Currie 2003a, b; Funston *et al.* 2021). Given that some other tyrannosaurids like *Daspletosaurus* spp., *Tyrannosaurus rex* and *Zhuchengtyrannus magnus*

had relative mandibular depths that are no different from what is observed in adults of *Tarbosaurus bataar* (Currie 2003b; Hurum & Sabath 2003; Hone *et al.* 2011), disproportionate increase in the depth of the posterior part of the dentary is probably more widespread within the clade.

In *Gorgosaurus libratus*, the maxillary fenestra is small, and is widely separated from the antorbital fossa by a bony apron (Currie 2003b). This morphology remained constant through the growth series of this taxon (Carr 1999; Currie 2003b; Voris *et al.* 2022). In *Tyrannosaurus rex*, young individuals have a small maxillary fenestra that is widely separated from the antorbital fossa, similar to *Gorgosaurus libratus* (Carr 1999, 2020; Carr & Williamson 2004). In immature *Tarbosaurus bataar*, however, the maxillary fenestra is widely separated from the antorbital fossa, even though it is large and is no different in relative size compared to adults. It appears that it just approached the anteroventral corner of the antorbital fossa as the animal grew, like adults of *Tyrannosaurus rex* (Carr 1999, 2020; Currie 2003b; Carr & Williamson 2004; Tsuihiji *et al.* 2011). The recognition of little change in relative size of the maxillary fenestra during growth in *Tarbosaurus bataar* reaffirms some of the previous observations (Currie & Dong 2001; Larson 2013) and provides quantitative support to them. An early emergence of an enlarged maxillary fenestra in the growth of *Tarbosaurus bataar* may suggest predisplacement peramorphosis occurred in the development of this feature in this taxon (Carr 2011). Of note, in their description of MPC-D 107/7, a two- to three-year-old *Tarbosaurus bataar*, Tsuihiji *et al.* (2011) noted that while the length of the maxillary fenestra is longer than the height in the immature growth stages of this taxon, the height is equal to the relative length in adults. This growth pattern was suggested to be a unique feature of *Tarbosaurus bataar* (Tsuihiji *et al.* 2011). In regression analysis of Procrustes coordinates onto log CS for *Tarbosaurus bataar* maxillae of this work, however, no clear trend of the relative increase of the height of the maxillary fenestra is observed during growth. Given the broad range of variation in the proportions of the maxillary fenestra in other tyrannosaurids like *Daspletosaurus* spp., or *Tyrannosaurus rex* (Carpenter 1990; Carr *et al.* 2017; Delcourt 2017), this trait may have simply been a part of individual variation that is unrelated to growth in *Tarbosaurus bataar*.

Analysis of the frontal bone shape changes indicates that as the length of the bone increased, the prefrontolacrimal process widened, and its anterior tip became hooked medially in *Tarbosaurus bataar*. Such ontogenetic variation is noted in *Tyrannosaurus*

rex by Carr (2020), and this observation suggests this growth pattern is shared between these two taxa. This pattern might be unique to the *Tarbosaurus bataar* + *Tyrannosaurus rex* clade, because in many other tyrannosaurids (*Gorgosaurus libratus*, *Teratophoneus curriei*), the prefrontolacrimal process is narrow and points anteriorly (Voris et al. 2022; Yun 2022). In *Daspletosaurus* spp., the process is wide, but points anterolaterally (Voris et al. 2022).

Intraspecific variation of craniomandibular anatomy of Tarbosaurus bataar

Given the limited sample size, it is not possible to fully assess shape changes associated with ontogeny in *Tarbosaurus bataar*. While some aspects of the craniomandibular variation observed in this study may be attributable to differential allometry, the absence of significant correlations between many PCs and size suggests that much of the variation is better interpreted as intraspecific. However, future analyses incorporating a larger number of specimens may show some variations discussed here are indeed linked to growth. PC2 of the dentary, which describes the shape of the anterodorsal tip and the anterior margin of the bone, is not correlated with size. The differences in the form of the anterior margins of the dentaries among tyrannosaurids might have taxonomic significance (Mallon et al. 2020), but it was argued that a considerable amount of intraspecific variation is present about this feature (Yun 2020a). Indeed, significant individual variation in the morphology of the dentary, including the anterior part, was previously reported in adults of *Tyrannosaurus rex* (Carpenter 1990). The results of the analyses in this work, may eliminate allometry or ontogeny as explanations for the variable shapes between different tyrannosaurid individuals.

PC2 for the morphometric analysis of the maxilla shape, is mainly about the relative position of the antorbital fossa along the anteroposterior axis of the bone, and is not correlated with size. The positions of the antorbital fossae would affect the relative lengths of the subcutaneous regions that are anterior to them. Some tyrannosaurid maxillae have truncated anterior regions, and although it has been argued that such morphological differences indicate taxonomic distinction (Carpenter 1990), it is now recognized that various individuals of *Daspletosaurus* spp., *Gorgosaurus libratus*, and *Tyrannosaurus rex* have such morphologies (Carr & Williamson 2000). Results of this work may imply that intraspecific variation in *Tarbosaurus bataar* is largely similar to those of North American tyrannosaurids.

PC2 for the shape of the jugal is not correlated with the size, and mostly describes the relative length of the ventral margin of the orbit. Similar intraspecific variation is present among adults of *Tyrannosaurus rex*: in some specimens (LACM 23844), the region is narrow whereas it is wide in other specimens (AMNH 5027, TMP 81.6.1; Carpenter 1990, fig. 10.1). Considering that *Allosaurus* also shows the same variation that is unrelated to allometry (Carpenter 2010), such variation might have been common among large theropods.

PC2 regarding the shape of the lacrimal is mostly associated with the relative length of the anterior ramus, and it lacks correlation with size. Intraspecific variation of the relative length of this region appears to be present in *Allosaurus* (Carpenter 2010, figs 4, 5), suggesting this might be another case of a widespread pattern of individual variation among large-bodied theropods. Apparently, this variation in the lacrimal is reflected in that of the nasal: PC1 for the nasal shape mostly describes the position of the lacrimal facet, and it is not correlated with size.

PC2 of the postorbital shape analysis mostly describes the degree of the ventral curvature of the posterior ramus, which contacts the squamosal in intact skulls (Currie 2003b). Paulina-Carabajal et al. (2021) suggested that the nature of the contact between the postorbital and the squamosal is polymorphic in *Gorgosaurus libratus*, *Tarbosaurus bataar* and *Tyrannosaurus rex*, but Voris et al. (2022) considered this to be monomorphic (i.e., different specimens of the same taxon exhibit a constant morphology). The results of this work lend support to the argument of Paulina-Carabajal et al. (2021), and suggest caution is needed about the usage of this feature to establish taxonomic identity of controversial specimens. Indeed, similar individual variation is present in *Allosaurus* (Carpenter 2010). Given that all the specimens examined in that work are from a single locality of the upper part of the Morrison Formation, they are likely monospecific (Smyth et al. 2020). This indicates a polymorphic nature of the postorbital-squamosal contact, exemplified by *Allosaurus* (Carpenter 2010) and tyrannosaurids such as *Tarbosaurus bataar*, suggest this is a common pattern among large theropods.

PC1 for the shape analysis of the quadratojugal is mostly associated with the broadness of the midheight region and the depth of the anterior process, and it is not correlated with the size. Although the intraspecific variation of the quadratojugal has received little attention in the literature, considerable variation in various cranial bones within a single population of

Allosaurus (Carpenter 2010) provisionally suggests almost every single bone in the entire theropod skull exhibited a substantial degree of individual variation (Smyth *et al.* 2020), while some of them may represent taphonomic distortions (Kammerer *et al.* 2020). Indeed, it appears that considerable variation in the morphology of the quadratojugal is present among adult *Tyrannosaurus rex* (Carpenter 1990, fig. 10.1; Warshaw & Fowler 2022). Therefore, it is no surprise that the quadratojugal of *Tarbosaurus bataar* exhibited significant intraspecific variability.

PC2 for the frontal shape analysis mostly describes the orientation of the medial portion of the dorsotemporal ridge, and the shape of the area between the postorbital buttress and the posterior shelf. Considerable variation in the orientation of the anterior edge of the dorsotemporal fossa is reported in *Daspletosaurus* spp. and *Tyrannosaurus rex* (Carr *et al.* 2017; Voris *et al.* 2020); the results of this work suggest this was the case for *Tarbosaurus bataar* as well. The region between the postorbital buttress and the posterior shelf is subject to ontogenetic and individual variation in tyrannosaurids (Carr & Williamson 2004; Lehman & Wick 2013; Yun 2020b, 2023), and this paper shows that this was also true for *Tarbosaurus bataar*. This suggests caution must be exercised when using this character to make taxonomic distinctions (McDonald *et al.* 2018; Yun 2020b, c).

PC2 regarding the shape of the parietal is mostly associated with the length and shape of the median spur that separates the frontals posteriorly, and no correlation between it and size was found. In adults of *Tyrannosaurus rex*, the spur is relatively broad and wedge-like in some specimens, whereas in others it is relatively short and narrow (Carr 2020). Results of this work suggest this region of the skull is subject to a high degree of intraspecific variation in *Tarbosaurus bataar* as well and calls into question of the usage of the shape of this character in diagnosing tyrannosaurids (Fiorillo & Tykoski 2014; Yun 2022; Perry 2023).

PC1 regarding surangular morphology is mostly associated with the size and the position of the surangular foramen, and it is not correlated with size. Although diminutive size of the posterior surangular foramen is sometimes used as an autapomorphy of *Tarbosaurus bataar* (Holtz 2004; Tsuihiji *et al.* 2011), the results of this work imply polymorphism of this character within this taxon. Indeed, at least one adult *Tarbosaurus bataar* has a significantly enlarged surangular foramen (ZPAL MgD-I/4; Hurum & Sabath 2003, fig. 1) compared to other individuals of this taxon, indicating the polymorphic nature of this character is likely real (e.g. PIN 551-3; Carr *et al.* 2022, fig. 2).

A bivariate linear regression analysis of Słowiak-Morkovina *et al.* (2024) also found no clear evidence for relatively diminutive size of the posterior surangular foramen of *Tarbosaurus bataar* compared with other tyrannosaurids, and the polymorphic nature of this character has been noted by these authors as well (Słowiak-Morkovina *et al.* 2024, p.34). Furthermore, considering the fact that the posterior surangular foramen of tyrannosaurids is most likely a result of bone resorption induced by a pneumatic diverticulum (Gold *et al.* 2013), it may be no surprise that the size, or even the number of the foramen varied between individuals (Słowiak-Morkovina *et al.* 2024).

A possibility of polymorphism in the size of the surangular foramen of *Tarbosaurus bataar*, may bear some implications about the taxonomic validity of the controversial tyrannosaurid taxon, *Raptorex kriegsteini*. Initially, *Raptorex kriegsteini* was erected as an early-diverging tyrannosauroid with a tyrannosaurid-like bauplan, based on incorrect assumptions that the holotype (LH PV18) is a subadult and originated from the early Cretaceous Yixian Formation of China (Serenó *et al.* 2009). Later, it turned out that the holotype is actually from the upper Cretaceous Nemegt Formation of Mongolia, and represents a two- to three-year-old juvenile tyrannosaurine (Fowler *et al.* 2011). Based on this information, this taxon has usually been attributed to a juvenile *Tarbosaurus bataar* (Fowler *et al.* 2011; Snively *et al.* 2019; Mallon *et al.* 2020), although other studies have argued for the distinctiveness of this taxon (Tsuihiji *et al.* 2011; Carr 2022). One of the grounds for claiming LH PV18 is not a juvenile *Tarbosaurus bataar* in Tsuihiji *et al.* (2011), is that the posterior surangular foramen of this specimen is relatively enlarged compared to that of a similarly-sized, definitive juvenile *Tarbosaurus bataar* (MPC-D 107/7). However, if the size of the posterior surangular foramen is polymorphic in *Tarbosaurus bataar*, this character would be insufficient to be used to distinguish *Raptorex kriegsteini* from this taxon. Additionally, at least some of the characters that Carr (2022) used to support the validity of *Raptorex kriegsteini* deserve some commentary. Carr (2022) noted that LH PV18 possesses an unusual concavity at the anterolateral corner of the dorsotemporal fossa of the frontal that is not seen in other tyrannosaurids, but such a feature is present in at least one tyrannosaurid individual (UMNH VP 16690) that has been assigned to *Teratophoneus curriei* (Loewen *et al.* 2013, fig. 3E). As the holotype of that taxon (BYU 8120/9396, in part) lacks such a feature (Yun 2022), the presence/absence of

this character may alternatively be interpreted as intraspecific variation within tyrannosaurids. Lastly, Carr (2022) noted that LH PV18 lacks a key autapomorphy (the subcutaneous flange of the maxilla) of *Tarbosaurus bataar* (Carr & Williamson 2010; Carr *et al.* 2022). However, at least some specimens (MPC-D 100/77, PIN 551-1, 553-1) referred to that taxon also do not possess such a feature (Carr 2005, p.685), raising a possibility of polymorphism of this character. Overall, these may suggest that the differences between *Raptorex kriegsteini* and *Tarbosaurus bataar* are fewer than previously recognized, and that the former belongs to the latter taxon. However, it is probably best to keep these taxa separate, as at least some characters (extremely thin, nearly straight ventral ramus of the lacrimal, distinct sub-orbital ligament scar, and unusually tall anteroventral ala of the lacrimal) do seem to be unique to LH PV18 (Tsuihiji *et al.* 2011; Carr 2022). Furthermore, BYU 8120/9396 and UMNH VP 16690 may pertain to different taxa, as it is possible that not all tyrannosaurid material from the Kaiparowits Formation are referable to a single taxon (Titus *et al.* 2023). Ultimately, numerous undescribed specimens of *Tarbosaurus bataar* (Hurum & Sabath 2003; Currie 2016; Jerzykiewicz *et al.* 2021; Lee *et al.* 2023) may resolve this problem by either refuting or corroborating their synonymy.

Collectively, these results suggest that non-allometric variations in craniomandibular bones of *Tarbosaurus bataar* are largely in accordance with those of other tyrannosaurids or large-bodied theropods. At present, it is not clear what factors contributed to these differences, and they could reflect simple individual variation, sexual dimorphism, and perhaps taxonomic variations or even in a low degree taphonomic distortions. Obviously, it would be difficult to attribute the wide range of variation in different bones as the result of just one of these potential factors, and it is possible that more than one may have contributed. Unfortunately, the current sample size is simply too small to say whether any factor is plausible or not. Even the sample size as large as 100 may fail to detect sexual dimorphism as great as 28% (Mallon 2017). The work of Hone & Mallon (2017) found that the sample sizes of at least 15 and 35 individuals per sex are required to statistically detect sexual dimorphism for organisms exhibiting rhea and crocodile dimorphism respectively. Furthermore, even in cases where sufficient sample sizes are present, statistically demonstrating sexual dimorphism is extremely difficult without a priori knowledge of sexes, or obvious sex-specific

characters (Hone *et al.* 2020). Given this situation, it may be more difficult to find variation at the species level in analyses based on small sample sizes (e.g. Carr *et al.* 2022). To summarize, at present, it cannot be said for certain whether these variations are simply intraspecific, related to sex, or even suggest taxonomic differences. Only the description of a sufficient number of additional specimens, and their inclusion in the morphometric analyses, will ultimately resolve this problem.

Conclusions

Geometric morphometrics suggest the ontogenetic changes in the skull structure of *Tarbosaurus bataar* include deepening of the craniomandibular elements, broadening of the area where the jaw adductor musculature attached onto the skull roof (frontal), and increase in size of the cornual processes of the postorbital and the jugal. Such ontogenetic trajectory is similar to that of North American tyrannosaurids, particularly *Tyrannosaurus rex*, and the results of this work reaffirm and supplement the previous hypothesis that overall sequence of growth changes in craniomandibular anatomy of tyrannosaurids is fairly conservative within this clade. Most of these growth changes are presumably related to structural strengthening of the skull and increase of the bite force through ontogeny. Finally, although much of the variation in the skull and lower jaw of *Tarbosaurus bataar* appears to be due to growth-related changes, a large amount of variation is found to be not correlated with the size. These variations may be due to simple individual variation, sexual dimorphism, taxonomic variation, or deformation through taphonomic processes, and it is expected that the relative significance of each variation has to be clarified through future descriptive studies of multiple *Tarbosaurus bataar* specimens.

Acknowledgements.- C.-G. Yun thanks Denise Crampton and Christian Foth, for the detailed guidance about geometric morphometry and related software. RD and PJC thank Khishigjav Tsogtbaatar and Ulziitseren Sanjaadash (Mongolian Paleontological Center) for accessing the collection in Ulaanbaatar. RD also thanks Hussam El Dine Zaher and Erika Hingst-Zaher for supervising his PhD thesis, and FAPESP (2012/09370-2; 2021/12231-3) for funding. Numerous *Tarbosaurus* specimens were collected, measured and photographed by PJC while on citizen science expeditions of Nomadic Expeditions, and Mongolia Quest, and the Korea-Mongolia International Dinosaur Project. These expeditions were funded amongst others by grants from the Dinosaur Research Institute (Calgary, Canada), Hwaseong City (South Korea), and NSERC (Discovery Grant RGPIN-2017-04715 to PJC). This manuscript was improved by insightful comments from an anonymous reviewer, and the editor Peter Doyle (London South Bank University, UK).

Supplementary online material

Supplementary Online Material 1. List of specimens used in the analyses, with sources of images.

Supplementary Online Material 2. List of landmarks and semi-landmark description.

Supplementary Online Material 3. MorphoJ and tps files including all shapes and analyses.

References

- Adams, D.C., Rohlf, F.J. & Slice, D.E. 2013: A field comes of age: geometric morphometrics in the 21st century. *Hystrix* 24, 7–14. <https://doi.org/10.4404/hystrix-24.1-6283>
- Bates, K.T. & Falkingham, P.L. 2012: Estimating maximum bite performance in *Tyrannosaurus rex* using multi-body dynamics. *Biology Letters* 8, 660–664. <https://doi.org/10.1098/rsbl.2012.0056>
- Bhullar, B.A.S., Marugán-Lobón, J., Racimo, F., Bever, G.S., Rowe, T.B., Norell, M.A. & Abzhanov, A. 2012: Birds have paedomorphic dinosaur skulls. *Nature* 487, 223–226. <https://doi.org/10.1038/nature11146>
- Bookstein, F.L. 1991: *Morphometric Tools for Landmark Data*. Cambridge University Press, Cambridge.
- Brown, C.M. & Vavrek, M.J. 2015: Small sample sizes in the study of ontogenetic allometry; implications for palaeobiology. *PeerJ* 3, e818. <https://doi.org/10.7717/peerj.818>
- Brusatte, S.L., Benson, R.B.J. & Xu, X. 2010: The evolution of large-bodied theropod dinosaurs during the Mesozoic in Asia. *Journal of Iberian Geology* 36, 275–296.
- Brusatte, S.L. & Carr, T.D. 2016: The phylogeny and evolutionary history of tyrannosaurid dinosaurs. *Scientific Reports* 6, 20252. <https://doi.org/10.1038/srep20252>
- Brusatte, S.L., Carr, T.D. & Norell, M.A. 2012a: The osteology of *Alioramus*, a gracile and long-snouted tyrannosaurid (Dinosauria: Theropoda) from the Late Cretaceous of Mongolia. *Bulletin of the American Museum of Natural History* 366, 1–197. <https://doi.org/10.1206/770.1>
- Brusatte, S.L., Sakamoto, M., Montanari, S. & Harcourt Smith, W.E.H. 2012b: The evolution of cranial form and function in theropod dinosaurs: insights from geometric morphometrics. *Journal of Evolutionary Biology* 25, 365–377. <https://doi.org/10.1111/j.1420-9101.2011.02427.x>
- Campione, N.E. & Evans, D.C. 2011: Cranial growth and variation in Edmontosaurs (Dinosauria: Hadrosauridae): implications for latest Cretaceous megaherbivore diversity in North America. *PLoS One* 6, e25186. <https://doi.org/10.1371/journal.pone.0025186>
- Carpenter, K. 1990: Variation in *Tyrannosaurus rex*, 141–145. In: Carpenter, K. & Currie, P.J. (Eds), *Dinosaur Systematics: Perspectives and Approaches*, Cambridge University Press, Cambridge.
- Carpenter, K. 1992: Tyrannosaurids (Dinosauria) of Asia and North America, 250–268. In: Mateer, N.J. & Chen Pei-Ji (Eds), *Aspects of Nonmarine Cretaceous Geology*, China Ocean Press, Beijing.
- Carpenter, K. 2010: Variation in a population of Theropoda (Dinosauria): *Allosaurus* from the Cleveland-Lloyd Quarry (Upper Jurassic), Utah, USA. *Paleontological Research* 14, 250–259. <https://doi.org/10.2517/1342-8144-14.4.250>
- Carr, T.D. 1999: Craniofacial ontogeny in Tyrannosauridae (Dinosauria, Coelurosauria). *Journal of Vertebrate Paleontology* 19, 497–520. <https://doi.org/10.1080/02724634.1999.10011161>
- Carr, T.D. 2005: *Phylogeny of Tyrannosauroida (Dinosauria: Coelurosauria) with Special Reference to North American Forms*. Unpublished Ph.D. Thesis, University of Toronto, Toronto.
- Carr, T.D. 2011: A comparative study of ontogeny between derived tyrannosauroids: evidence for heterochrony. *Journal of Vertebrate Paleontology, Program and Abstracts 2011*, 84A.
- Carr, T.D. 2020: A high-resolution growth series of *Tyrannosaurus rex* obtained from multiple lines of evidence. *PeerJ* 8, e9192. <https://doi.org/10.7717/peerj.9192>
- Carr, T.D. 2022: A reappraisal of tyrannosauroid fossils from the Iren Dabasu Formation (Coniacian–Campanian), Inner Mongolia, People's Republic of China. *Journal of Vertebrate Paleontology* 42, e2199817. <https://doi.org/10.1080/02724634.2023.2199817>
- Carr, T.D. & Williamson, T.E. 2000: A review of Tyrannosauridae (Dinosauria, Coelurosauria) from New Mexico. *New Mexico Museum of Natural History and Science Bulletin* 17, 113–146.
- Carr, T.D. & Williamson, T.E. 2004: Diversity of late Maastrichtian Tyrannosauridae (Dinosauria: Theropoda) from western North America. *Zoological Journal of the Linnean Society* 142, 479–523. <https://doi.org/10.1111/j.1096-3642.2004.00130.x>
- Carr, T.D. & Williamson, T.E. 2010: *Bistahieversor sealeyi*, gen. et sp. nov., a new tyrannosauroid from New Mexico and the origin of deep snouts in Tyrannosauroida. *Journal of Vertebrate Paleontology* 30, 1–16. <https://doi.org/10.1080/02724630903413032>
- Carr, T.D., Napoli, J.G., Brusatte, S.L., Holtz, T.R., Hone, D.W.E., Williamson, T.E. & Zanno, L.E. 2022: Insufficient evidence for multiple species of *Tyrannosaurus* in the latest Cretaceous of North America. *Evolutionary Biology* 49, 327–341. <https://doi.org/10.1007/s11692-022-09573-1>
- Carr, T.D., Varricchio, D.J., Sedlmayr, J.C., Roberts, E.M. & Moore, J.R. 2017: A new tyrannosaur with evidence for anagenesis and a crocodile-like facial sensory system. *Scientific Reports* 7, 44942. <https://doi.org/10.1038/srep44942>
- Carr, T.D., Williamson, T.E. & Schwimmer, D.R. 2005: A new genus and species of tyrannosauroid from the Late Cretaceous (Middle Campanian) Demopolis Formation of Alabama. *Journal of Vertebrate Paleontology* 25, 119–143. [https://doi.org/10.1671/0272-4634\(2005\)025\[0119:ANGASO\]2.0.CO;2](https://doi.org/10.1671/0272-4634(2005)025[0119:ANGASO]2.0.CO;2)
- Cooke, S.B. & Terhune, C.E. 2015: Form, function, and geometric morphometrics. *The Anatomical Record* 298, 5–28. <https://doi.org/10.1002/ar.23065>
- Coppock, C.C., Powers, M.J., Voris, J.T., Sharpe, H.S. & Currie, P.J. 2024: Immature *Daspletosaurus* sp. specimens from the Dinosaur Park Formation provide insight into ontogenetically invariant tyrannosaurid cranial morphology. *Canadian Journal of Earth Sciences* 61, 1227–1239. <https://doi.org/10.1139/cjes-2024-0083>
- Currie, P.J. 2003a: Cranial anatomy of tyrannosaurid dinosaurs from the Late Cretaceous of Alberta, Canada. *Acta Palaeontologica Polonica* 48, 191–226.
- Currie, P.J. 2003b: Allometric growth in tyrannosaurids (Dinosauria: Theropoda) from the Upper Cretaceous of North America and Asia. *Canadian Journal of Earth Sciences* 40, 651–665. <https://doi.org/10.1139/e02-083>
- Currie, P.J., and Y. Azuma. 2006. New specimens, including a growth series, of *Fukuiraptor* (Dinosauria, Theropoda) from the Lower Cretaceous Kitadani Quarry of Japan. *Journal of the Paleontological Society of Korea* 22, 173–193.
- Currie, P.J. 2016: Dinosaurs of the Gobi: Following in the footsteps of the Polish-Mongolian Expeditions. *Palaentologia Polonica* 67, 83–100. http://dx.doi.org/10.4202/pp.2016.67_083
- Currie, P.J. & Dong, Z.M. 2001: New information on *Shanshanosaurus huoyanshanensis*, a juvenile tyrannosaurid (Theropoda, Dinosauria) from the Late Cretaceous of China. *Canadian Journal of Earth Sciences* 38, 1729–1737. <https://doi.org/10.1139/e01-042>
- Delcourt, R. 2016: *Evolução morfológica de Ceratosauria e Tyrannosauroida (Dinosauria: Theropoda)*. Unpublished Ph.D. Thesis, Universidade de São Paulo, São Paulo.

- Delcourt, R. 2017: A subadult maxilla of a Tyrannosauridae from the Two Medicine Formation, Montana, United States. *Papéis Avulsos de Zoologia* 57, 113–118. <https://doi.org/10.11606/0031-1049.2017.57.09>
- Fiorillo, A.R. & Tykoski, R.S. 2014: A diminutive new tyrannosaur from the top of the world. *PLoS One* 9, e91287. <https://doi.org/10.1371/journal.pone.0091287>
- Foster, W., Brusatte, S.L., Carr, T.D., Williamson, T.E., Yi, L. & Lü, J. 2022: The cranial anatomy of the long-snouted tyrannosaurid dinosaur *Qianzhousaurus sinensis* from the Upper Cretaceous of China. *Journal of Vertebrate Paleontology* 41, e1999251. <https://doi.org/10.1080/02724634.2021.1999251>
- Foth, C. & Rauhut, O.W.M. 2013: Macroevolutionary and morphofunctional patterns in theropod skulls: A morphometric approach. *Acta Palaeontologica Polonica* 58, 1–16. <https://doi.org/10.4202/app.2011.0145>
- Foth, C., Hedrick, B.P. & Ezcurra, M.D. 2016: Cranial ontogenetic variation in early saurischians and the role of heterochrony in the diversification of predatory dinosaurs. *PeerJ* 4, e1589. <https://doi.org/10.7717/peerj.1589>
- Fowler, D.W., Woodward, H.M., Freedman, E.A., Larson, P.L. & Horner, J.R. 2011: Reanalysis of ‘*Raptorex kriegsteini*’: a juvenile tyrannosaurid dinosaur from Mongolia. *PLoS One* 6, e21376. <https://doi.org/10.1371/journal.pone.0021376>
- Funston G.F., Powers M.J., Whitebone S.A., Brusatte S.L., Scannella J.B., Horner J.R. & Currie P.J. 2021: Baby tyrannosaurid bones and teeth from the Late Cretaceous of western North America. *Canadian Journal of Earth Sciences* 58, 756–777. <https://doi.org/10.1139/cjes-2020-0169>
- Gates, T.A., Organ, C. & Zanno, L.E. 2016: Bony cranial ornamentation linked to rapid evolution of gigantic theropod dinosaurs. *Nature Communications* 7, 12931. <https://doi.org/10.1038/ncomms12931>
- Gignac, P.M. & Erickson, G.M. 2017: The biomechanics behind extreme osteophagy in *Tyrannosaurus rex*. *Scientific Reports* 7, 2012. <https://doi.org/10.1038/s41598-017-02161-w>
- Gold, M.E.L., Brusatte, S.L. & Norell, M.A. 2013: The cranial pneumatic sinuses of the tyrannosaurid *Alioramus* (Dinosauria: Theropoda) and the evolution of cranial pneumaticity in theropod dinosaurs. *American Museum Novitates* 3790, 1–46. <https://doi.org/10.1206/3790.1>
- Hedrick, B. 2023: Dots on a screen: The past, present, and future of morphometrics in the study of nonavian dinosaurs. *The Anatomical Record* 306, 1896–1917. <https://doi.org/10.1002/ar.25183>
- Henderson, D.M. 2002: The eyes have it: the sizes, shapes, and orientations of theropod orbits as indicators of skull strength and bite force. *Journal of Vertebrate Paleontology* 22, 766–778. [https://doi.org/10.1671/0272-4634\(2002\)022\[0766:TEHITS\]2.0.CO;2](https://doi.org/10.1671/0272-4634(2002)022[0766:TEHITS]2.0.CO;2)
- Holtz, T.R., Jr. 2004: Tyrannosauroida, 111–136. In: Weishampel, D.B., Dodson, P. & Osmólska, H. (Eds), *The Dinosauria*, second edition. University of California Press, Berkeley.
- Hone, D.W.E. & Mallon, J.C. 2017: Protracted growth impedes the detection of sexual dimorphism in non-avian dinosaurs. *Palaeontology* 60, 535–545. <https://doi.org/10.1111/pala.12298>
- Hone, D.W.E., Mallon, J.C., Hennessey, P. & Witmer, L.M. 2020: Ontogeny of a sexually selected structure in an extant archosaur *Gavialis gangeticus* (Pseudosuchia: Crocodylia) with implications for sexual dimorphism in dinosaurs. *PeerJ* 8, e9134. <https://doi.org/10.7717/peerj.9134>
- Hone, D.W.E., Naish, D. & Cuthill, I.C. 2012: Does mutual sexual selection explain the evolution of head crests in pterosaurs and dinosaurs? *Lethaia* 45, 139–156. <https://doi.org/10.1111/j.1502-3931.2011.00300.x>
- Hone, D.W.E., Wood, D. & Knell, R.J. 2016: Positive allometry for exaggerated structures in the ceratopsian dinosaur *Protoceratops andrewsi* supports socio-sexual signaling. *Palaeontologia Electronica* 19, 1–13. <https://doi.org/10.26879/591>
- Hone, D.W.E., Wang, K., Sullivan, C., Zhao, X., Chen, S., Li, D., Ji, S., Ji, Q. & Xu X. 2011: A new, large tyrannosaurine theropod from the Upper Cretaceous of China. *Cretaceous Research* 32, 495–503. <https://doi.org/10.1016/j.cretres.2011.03.005>
- Hurum, J.H. & Currie, P.J. 2000: The crushing bite of tyrannosaurids. *Journal of Vertebrate Paleontology* 20, 619–621. [https://doi.org/10.1671/0272-4634\(2000\)020\[0619:TCBOT\]2.0.CO;2](https://doi.org/10.1671/0272-4634(2000)020[0619:TCBOT]2.0.CO;2)
- Hurum, J.H. & Sabath, K. 2003: Giant theropod dinosaurs from Asia and North America: Skulls of *Tarbosaurus bataar* and *Tyrannosaurus rex* compared. *Acta Palaeontologica Polonica* 48, 161–190.
- Jerzykiewicz, T., Currie, P.J., Fanti, F. & Lefeld, J. 2021: Lithobiotopes of the Nemegt Gobi Basin. *Canadian Journal of Earth Sciences* 58, 829–851. <https://doi.org/10.1139/cjes-2020-0148>
- Johnson-Ransom, E., Li, F., Xu, X., Ramos, R., Midzuk, A. J., Thon, U., Atkins-Weltman, K. & Snively, E. 2024: Comparative cranial biomechanics reveal that Late Cretaceous tyrannosaurids exerted relatively greater bite force than in early-diverging tyrannosauroids. *The Anatomical Record* 307, 1897–1917. <https://doi.org/10.1002/ar.25326>
- Kammerer, C.F., Deutsch, M., Lungmus, J.K. & Angielczyk, K.D. 2020: Effects of taphonomic deformation on geometric morphometric analysis of fossils: a study using the dicynodont *Diictodon feliceps* (Therapsida, Anomodontia) *PeerJ* 8, e9925. <https://doi.org/10.7717/peerj.9925>
- Klingenberg, C.P. 2011: MorphoJ: an integrated software package for geometric morphometrics. *Molecular Ecology Resources* 11, 353–357. <https://doi.org/10.1111/j.1755-0998.2010.02924.x>
- Knapp, A., Knell, R.J. & Hone, D.W.E. 2021. Three-dimensional geometric morphometric analysis of the skull of *Protoceratops andrewsi* supports a socio-sexual signalling role for the ceratopsian frill. *Proceedings of the Royal Society B: Biological Sciences* 288, 20202938. <https://doi.org/10.1098/rspb.2020.2938>
- Larson, P.L. 2013: The case for *Nanotyrannus*, 15–53. In: Parrish, J.M., Molnar, R.E., Currie, P.J. & Koppelhus, E.B. (Eds), *Tyrannosaurid Paleobiology*. Indiana University Press, Bloomington.
- Lautenschlager, S. 2022: Functional and ecomorphological evolution of orbit shape in mesozoic archosaurs is driven by body size and diet. *Communications Biology* 5, 754. <https://doi.org/10.1038/s42003-022-03706-0>
- Lee, Y.-N., Jacobs, L.L., Currie, P.J. & Barsbold, R. 2023: Narrative of the Korea-Mongolia International Dinosaur Expeditions (KID) 2006–2010 with scientific results, 233–251. In: Lee, Y.-N. (Ed.), *Windows into Saurapsid and Synapsid Evolution*. Dinosaur Science Center Press.
- Lehman, T.M. & Wick, S.T. 2013: Tyrannosauroid dinosaurs from the Aguja Formation (Upper Cretaceous) of Big Bend National Park, Texas. *Earth and Environmental Science Transactions of the Royal Society of Edinburgh* 103, 471–485. <https://doi.org/10.1017/S1755691013000261>
- Loewen, M.A., Irmis, R.B., Sertich, J.W., Currie, P.J. & Sampson, S.D. 2013: Tyrant dinosaur evolution tracks the rise and fall of Late Cretaceous oceans. *PLoS One* 8, e79420. <https://doi.org/10.1371/journal.pone.0079420>
- Ma, W., Brusatte, S.L., Lü, J. and Sakamoto, M. 2020: The skull evolution of oviraptorosaurian dinosaurs: the role of niche-partitioning in diversification. *Journal of Evolutionary Biology* 33, 178–188. <https://doi.org/10.1111/jeb.13557>
- Maiorino, L., Farke, A.A., Kotsakis, T. & Piras, P. 2013: Is *Torosaurus Triceratops*? Geometric Morphometric Evidence of Late Maastrichtian Ceratopsid Dinosaurs. *PLoS One* 8, e81608. <https://doi.org/10.1371/journal.pone.0081608>
- Maiorino, L., Farke, A.A., Kotsakis, T. & Piras, P. 2015: Males Resemble Females: Re-Evaluating Sexual Dimorphism in *Protoceratops andrewsi* (Neoceratopsia, Protoceratopsidae). *PLoS One* 10, e0126464. <https://doi.org/10.1371/journal.pone.0126464>
- Maleev, E.A. 1955a: Gigantic carnivorous dinosaurs from Mongolia. *Doklady AN SSSR* 104, 634–637. [in Russian]

- Maleev, E.A. 1955b: New carnivorous dinosaurs from the Upper Cretaceous of Mongolia. *Doklady AN SSSR* 104, 779–782. [in Russian]
- Maleev, E.A. 1974: Gigantic carnosaurs of the family Tyrannosauridae. *Joint Soviet-Mongolian Palaeontological Expedition, Transactions* 1, 132–191. [in Russian]
- Mallon, J.C. 2017: Recognizing sexual dimorphism in the fossil record: Lessons from nonavian dinosaurs. *Paleobiology* 43, 495–507. <https://doi.org/10.1017/pab.2016.51>
- Mallon, J.C., Bura, J.R., Schumann, D. & Currie, P.J. 2020: A problematic tyrannosaurid (Dinosauria: Theropoda) skeleton and its implications for tyrannosaurid diversity in the Horseshoe Canyon Formation (Upper Cretaceous) of Alberta. *The Anatomical Record* 303, 673–690. <https://doi.org/10.1002/ar.24199>
- McDonald, A.T., Wolfe, D.G. & Dooley, A.C. 2018: A new tyrannosaurid (Dinosauria: Theropoda) from the Upper Cretaceous Menefee Formation of New Mexico. *PeerJ* 6, e5749. <https://doi.org/10.7717/peerj.5749>
- Mitteroecker, P., Gunz, P., Windhager, S. & Schaefer, K. 2013: A brief review of shape, form, and allometry in geometric morphometrics, with applications to human facial morphology. *Hystrix* 24, 59–66. <https://doi.org/10.4404/hystrix-24.1-6369>
- Molnar, R.E. 2013: A comparative analysis of reconstructed jaw musculature and mechanics of some large theropods, 177–193. In: Parrish, J.M., Molnar, R.E., Currie, P.J. & Koppelhus, E.B. (Eds), *Tyrannosaurid Paleobiology*. Indiana University Press, Bloomington.
- O’Higgins, P. & Johnson, D.R. 1988: The quantitative description and comparison of biological forms. *Critical Reviews in Anatomical Science* 1, 149–170.
- Olshevsky, G. & Ford, T.L. 1995: The origin and evolution of the Tyrannosauridae, part 2. *Dino Frontline* 6, 75–99. [in Japanese]
- Paul, G.S. 2008: The Extreme Lifestyles and Habits of the Gigantic Tyrannosaurid Superpredators of the Late Cretaceous of North America and Asia. In: Larson, P. & Carpenter, K. (Eds), *Tyrannosaurus rex, The Tyrant King*, 307–354. Indiana University Press, Bloomington.
- Paulina-Carabajal, A., Currie, P.J., Dudgeon, T.W., Larsson, H.C. & Miyashita, T. 2021. Two braincases of *Daspletosaurus* (Theropoda: Tyrannosauridae): anatomy and comparison. *Canadian Journal of Earth Sciences* 58, 885–910. <https://doi.org/10.1139/cjes-2020-0185>
- Perry, Z.R. 2023. A Reinterpretation of *Nanuqsaurus hoglundi* (Tyrannosauridae) from the Late Cretaceous Prince Creek Formation, Northern Alaska. Unpublished MSc Thesis, Department of Geosciences, University of Alaska, Fairbanks.
- Plateau, O. & Foth, C. 2020: Birds have peramorphic skulls, too: Anatomical network analyses reveal oppositional heterochronies in avian skull evolution. *Communications Biology* 3, 1–12. <https://doi.org/10.1038/s42003-020-0914-4>
- Polly, P. D. 2018. Geometric morphometrics, 1–5. In: López-Varela, S.L. (Ed.), *The Encyclopedia of Archeological Sciences*. John Wiley and Sons, Hoboken.
- Ratsimbaholison, N.O., Felice, R.N. & O’Connor, P.M. 2016: Ontogenetic changes in the craniomandibular skeleton of the abelisaurid dinosaur *Majungasaurus crenatissimus* from the Late Cretaceous of Madagascar. *Acta Palaeontologica Polonica* 61, 281–292. <http://dx.doi.org/10.4202/app.00132.2014>
- Rayfield, E.J. 2004: Cranial mechanics and feeding in *Tyrannosaurus rex*. *Proceedings of the Royal Society of London Series B* 271, 1451–1459. <https://doi.org/10.1098/rspb.2004.2755>
- Rohlf, F.J. 2015: The tps series of software. *Hystrix* 26, 9–12. <https://doi.org/10.4404/hystrix-26.1-11264>
- Rohlf, F.J. 2017a: tpsUtil, v. 1.74. Department of Ecology & Evolution, State University of New York, Stony Brook.
- Rohlf, F.J. 2017b: tpsDig, v. 2.30. Department of Ecology & Evolution, State University of New York, Stony Brook.
- Rohlf, F.J. & Marcus, L.F. 1993: A revolution morphometrics. *Trends in Ecology & Evolution* 8, 129–132. [https://doi.org/10.1016/0169-5347\(93\)90024-J](https://doi.org/10.1016/0169-5347(93)90024-J)
- Rowe, A.J. & Snively, E. 2022: Biomechanics of juvenile tyrannosaurid mandibles and their implications for bite force: evolutionary biology. *The Anatomical Record* 305, 373–392. <https://doi.org/10.1002/ar.24602>
- Rozhdestvensky, A.K. 1965: Growth changes and some problems of systematics of Asian dinosaurs. *Paleontologičeskij žurnal* 3, 95–109. [in Russian]
- Russell, D. 1970: Tyrannosaurs from the Late Cretaceous of western Canada. *National Museum Natural Sciences Publications in Palaeontology* 1, 1–34.
- Sakamoto, M. 2022: Estimating bite force in extinct dinosaurs using phylogenetically predicted physiological cross-sectional areas of jaw adductor muscles. *PeerJ* 10, e13731. <https://doi.org/10.7717/peerj.13731>
- Samman, T., Powell, G.L., Currie, P.J. & Hills, L.V. 2005. Morphometry of the teeth of western North American tyrannosaurids and its applicability to quantitative classification. *Acta Palaeontologica Polonica* 50, 757–776.
- Scannella J.B. & Horner J.R. 2011: ‘Nedoceratops’: An example of a transitional morphology. *PLoS One* 6, e28705. <https://doi.org/10.1371/journal.pone.0028705>
- Sereno, P.C., Tan, L., Brusatte, S.L., Kriegstein, H.J., Zhao, X. & Cloward, K. 2009: Tyrannosaurid skeletal design first evolved at small body size. *Science* 326, 418–422. <https://doi.org/10.1126/science.1177428>
- Sharpe, H.S., Wang, Y.Y., Dudgeon, T.W., Powers, M.J., Whitebone, S.A., Coppock, C.C., Dyer, A.D. & Sullivan, C. 2025: Skull morphology and histology indicate the presence of an unexpected buccal soft tissue structure in dinosaurs. *Journal of Anatomy*, 1–29. <https://doi.org/10.1111/joa.14242>
- Słowiak-Morkovina, J., Brusatte, S.L. & Szczygielski, T. 2024: Reassessment of the enigmatic Late Cretaceous theropod dinosaur, *Bagaraatan ostromi*. *Zoological Journal of the Linnean Society*. <https://doi.org/10.1093/zoolinnean/zlad169>.
- Smyth, R.S., Ibrahim, N. & Martill, D.M. 2020: *Sigilmassasaurus* is *Spinosaurus*: a reappraisal of African spinosaurines. *Cretaceous Research* 114, 104520. <https://doi.org/10.1016/j.cretres.2020.104520>
- Snively, E. & Russell, A. 2007: Functional variation of neck muscles and their relation to feeding style in Tyrannosauridae and other large theropod dinosaurs. *The Anatomical Record* 290, 934–957. <https://doi.org/10.1002/ar.20563>
- Snively, E., O’Brien, H., Henderson, D.M., Mallison, H., Surring, L.A., Burns, M.E., Holtz, T.R. Jr., Russell, A.P., Witmer, L.M., Currie, P.J., Hartman, S.A. & Cotton, J.R. 2019: Lower rotational inertia and larger leg muscles indicate more rapid turns in tyrannosaurids than in other large theropods. *PeerJ* 7, e6432. <https://doi.org/10.7717/peerj.6432>
- Sullivan, C. & Xu, X. 2017: Morphological diversity and evolution of the jugal in dinosaurs. *The Anatomical Record* 300, 30–48. <https://doi.org/10.1002/ar.23488>
- Therrien, F., Henderson, D. & Ruff, C.B. 2005: Bite me: biomechanical models of theropod mandibles and implications for feeding behavior, 179–237. In: Carpenter, K. (Ed.), *The Carnivorous Dinosaurs*. Indiana University Press, Bloomington.
- Therrien, F., Zelenitsky, D.K., Voris, J.T. & Tanaka, K. 2021: Mandibular force profiles and tooth morphology in growth series of *Albertosaurus sarcophagus* and *Gorgosaurus libratus* (Tyrannosauridae: Albertosaurinae) provide evidence for an ontogenetic dietary shift in tyrannosaurids. *Canadian Journal of Earth Sciences* 58, 812–828. <https://doi.org/10.1139/cjes-2020-017>
- Titus, A.L., Sertich, J.J.W., Irmis, R.B. & Loewen, M.A. 2023: Tyrannosaurid dinosaur diversity in middle and upper Campanian (Late Cretaceous) ecosystems of Laramidia: new information from the Kaiparowits Formation of southern Utah, USA. In: Hunt-Foster, R.K., Kirkland, J.I. & Loewen, M.A. (Eds), *14th Symposium on Mesozoic Terrestrial Ecosystems*

- and Biota. *The Anatomical Record* 306 (S1), 242–243. <https://doi.org/10.1002/ar.25219>
- Tsuihiji, T. 2010: Reconstructions of the axial muscle insertions in the occipital region of dinosaurs: evaluations of past hypotheses on Marginocephalia and Tyrannosauridae using the Extant Phylogenetic Bracket approach. *The Anatomical Record* 293, 1360–1386. <https://doi.org/10.1002/ar.21191>
- Tsuihiji, T., Watabe, M., Tsogtbaatar, K., Tsubamoto, T., Barsbold, R., Suzuki, S., Lee, A.H., Ridgely, R.C., Kawahara, Y. & Witmer, L.M. 2011: Cranial osteology of a juvenile specimen of *Tarbosaurus bataar* (Theropoda, Tyrannosauridae) from the Nemegt Formation (Upper Cretaceous) of Bugin Tsav, Mongolia. *Journal of Vertebrate Paleontology* 31, 497–517. <https://doi.org/10.1080/02724634.2011.557116>
- Voris, J.T., Zelenitsky, D.K., Therrien, F. & Currie, P.J. 2019: Reassessment of a juvenile *Daspletosaurus* from the Late Cretaceous of Alberta, Canada with implications for the identification of immature tyrannosaurids. *Scientific Reports* 9, 17801. <https://doi.org/10.1038/s41598-019-53591-7>
- Voris, J.T., Therrien, F., Zelenitsky, D.K. & Brown, C.M. 2020: A new tyrannosaurine (Theropoda: Tyrannosauridae) from the Campanian Foremost Formation of Alberta, Canada, provides insight into the evolution and biogeography of tyrannosaurids. *Cretaceous Research* 110, 104388. <https://doi.org/10.1016/j.cretres.2020.104388>
- Voris, J.T., Zelenitsky, D.K., Therrien, F., Ridgely, R.C., Currie, P.J. & Witmer, L.M. 2022: Two exceptionally preserved juvenile specimens of *Gorgosaurus libratus* (Tyrannosauridae, Albertosaurinae) provide new insight into the timing of ontogenetic changes in tyrannosaurids. *Journal of Vertebrate Paleontology* 41, e2041651. <https://doi.org/10.1080/02724634.2021.2041651>
- Wang, C. & Fang, Z. 2023: Ontogenetic variation and sexual dimorphism of beaks among four cephalopod species based on geometric morphometrics. *Animals* 13, 752. <https://doi.org/10.3390/ani13040752>
- Warshaw, E.A. & Fowler, D.W. 2022: A transitional species of *Daspletosaurus* Russell, 1970 from the Judith River Formation of eastern Montana. *PeerJ* 10, e14461. <https://doi.org/10.7717/peerj.14461>
- Yun, C.-G. 2020a: Corrections and comments on the taxonomic value of anatomical features of tyrannosaurid theropods. *The Anatomical Record* 303, 2788–2791. <https://doi.org/10.1002/ar.24458>
- Yun, C.-G. 2020b: A reassessment of the taxonomic validity of *Dynamoterror dynastes* (Theropoda: Tyrannosauridae). *Zooiversity* 54, 259–264. <https://doi.org/10.15407/zoo2020.03.259>
- Yun, C.-G. 2020c: A subadult frontal of *Daspletosaurus torosus* (Theropoda: Tyrannosauridae) from the Late Cretaceous of Alberta, Canada with implications for Tyrannosaurid Ontogeny and Taxonomy. *PalArch's Journal of Vertebrate Palaeontology* 17, 1–13.
- Yun, C.-G. 2022: Frontal bone anatomy of *Teratophoneus curriei* (Theropoda: Tyrannosauridae) from the Upper Cretaceous Kaiparowits Formation of Utah. *Acta Palaeontologica Romaniae* 18, 51–64. <https://doi.org/10.35463/j.apr.2022.01.06>
- Yun, C.-G. 2023: Probable juvenile frontal of *Daspletosaurus horneri* (Dinosauria: Theropoda) from the Two Medicine Formation of Montana, with implications for tyrannosaurid ontogeny. *Acta Palaeontologica Romaniae* 19, 3–11. <https://doi.org/10.35463/j.apr.2023.01.01>
- Yun, C.-G., Peters, G.F. & Currie, P.J. 2022: Allometric growth in the frontals of the Mongolian theropod dinosaur *Tarbosaurus bataar*. *Acta Palaeontologica Polonica* 67, 601–615. <https://doi.org/10.4202/app.00947.2021>